STYRELSEN FÖR

**VINTERSJÖFARTSFORSKNING**

WINTER NAVIGATION RESEARCH BOARD

Research Report No 132

Ville Valtonen

# DIRECT CALCULATION METHODS FOR ICE STRENGTHENED HULLS, PART III

Finnish Transport and Communications Agency

Finnish Transport Infrastructure Agency

Finland

Swedish Maritime Administration

Swedish Transport Agency

Sweden

Talvimerenkulun tutkimusraportit — Winter Navigation Research Reports
ISSN 2342-4303
ISBN 978-952-311-970-3

**FOREWORD**

In this report no 132, the Winter Navigation Research Board presents the results of HULLFEM III - Direct calculation methods for ice strengthened hulls, part III. This is the third and final research project in the series of developing direct calculation methods for the hull design of the Finnish-Swedish ice class rules. As an important result of the project a rule draft has been created. The background for this draft is contained in the totality of the research within the series HULLFEM I, II and III.

The Winter Navigation Research Board warmly thanks Ville Valtonen for this report.

Helsinki

March 2025

| | |
|---|---|
| Ville Häyrynen | Amund Lindberg |
| Finnish Transport and Communications Agency | Swedish Maritime Administration |
| Helena Orädd | Fredrik Hellsberg |
| Finnish Transport Infrastructure Agency | Swedish Transport Agency |

Aker Arctic

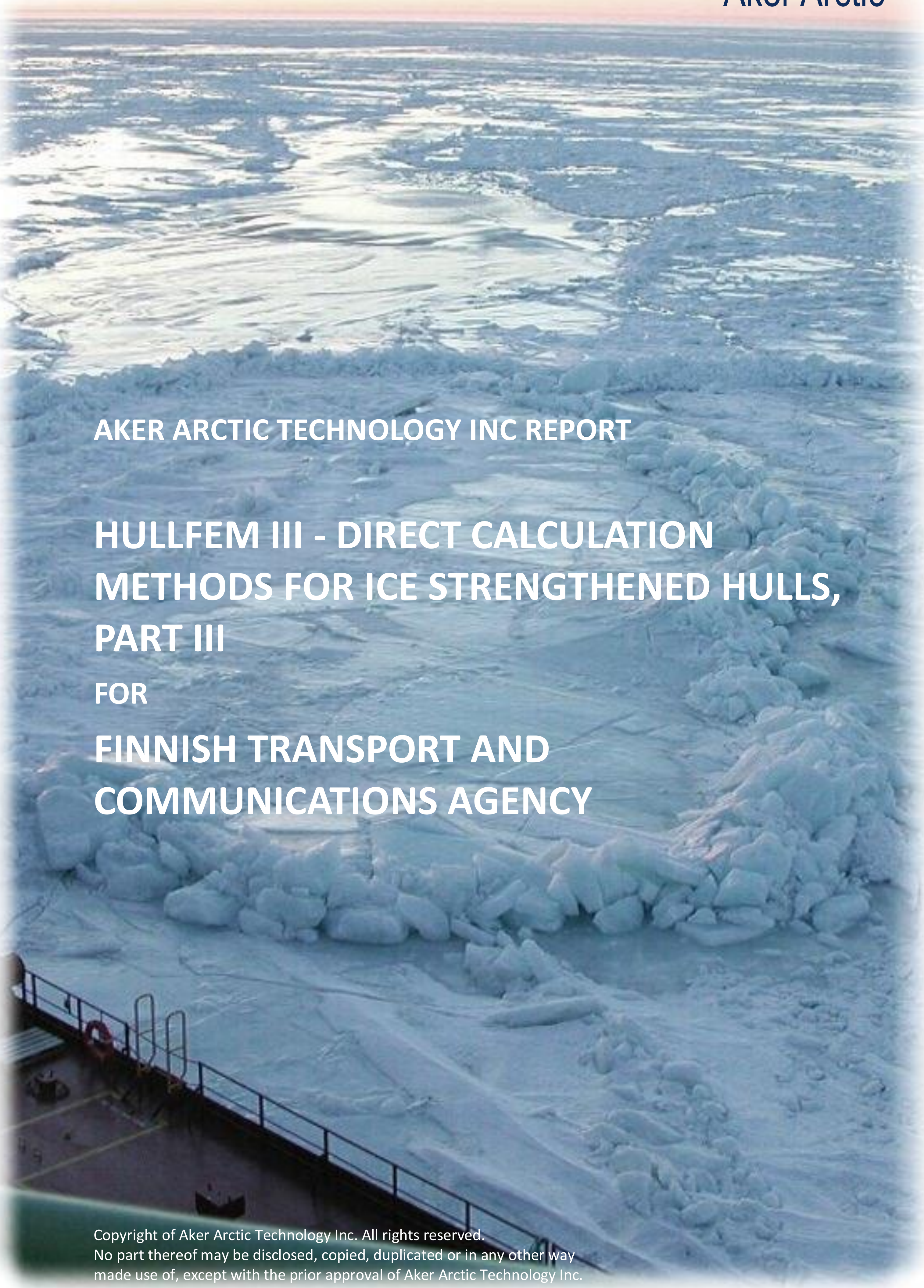

AKER ARCTIC TECHNOLOGY INC REPORT

# HULLFEM III - DIRECT CALCULATION METHODS FOR ICE STRENGHTHENED HULLS, PART III

FOR

# FINNISH TRANSPORT AND COMMUNICATIONS AGENCY

| **Name of document:** HULLFEM III - Direct calculation methods for ice strengthened hulls, part III | | | |
|---|---|---|---|
| **Document Responsible:** Ville Valtonen | | **Document Co-Author(s):** | |
| **Document Reviewer:** Oskar Veltheim | | **Document Approver:** Juuso Lindroos | |
| **Report number / Revision:** K560 / A | | **Status / Status Date:** Approved / 2024-12-17 | |
| **Client:** Winter Navigation Research Board / Ville Häyrynen | | | |
| **Revision remarks:** Final version | | | |

**Summary:**

In this report, the final part for the work to develop direct calculation method alternative for the hull section of the Finnish-Swedish Ice Class Rules is described. The acceptance criteria developed in earlier parts are refined to their final form and a rule draft is written.

An example bow is analyzed to ensure that the methodology that was studied in parallel midbody region in the previous projects is applicable to the shaped regions of the hull. The two main differences between the bow and the midbody are the higher ice load at the bow, and the shaped hull geometry. The results show that the proposed method is applicable to both prismatic and shaped hull regions and that the results do not differ significantly between these.

In addition to the bow analysis, some of the earlier analyses were refined, and couple of small additional analyses were made to answer the questions that arose during the Class society review of the rule proposal.

The results from the current and previous projects have been collected together, and from these the required design loads for the new rules have been developed, following the principles agreed with Traficom.

Using the knowledge basis from these three projects, a draft of the new rules is written for the use of direct calculations methods for the FSICR. The rule draft has been presented to Classification societies for commenting and updated and refined based on the comments received and are considered ready to be taken into use.

**Keywords:**

Finite Element Method (FEM); Non-linear; Finnish-Swedish ice class rules (FSICR)

| **Client reference:** | | **Project number:** | **Language:** |
|---|---|---|---|
| W24-5 HULLFEM III | | 31008 | English |
| **Pages, total:** | **Attachments:** | **Distribution list:** | **Confidentiality:** |
| 37 | | | Confidential |

# TABLE OF CONTENTS



# APPENDICES

# 1 INTRODUCTION

In the current Finnish-Swedish Ice Class Rules (FSICR) the direct calculation methods, such as finite element method (FEM) are in general not allowed for assessing the hull strength against ice loads, except specific cases mentioned in section 4.1. While the current prescriptive formulas have good service experience, they are somewhat limiting for the design.

The goal of the HULLFEM III project is to continue the work of HULLFEM I & II projects to gather a better understanding of using direct calculation methods in the case of ice loads. This work aims to form a solid foundation for expanding the rules with provisions for direct analysis. The main aims of this continuation project are to study an example bow and to write draft rules.

The example bow is analyzed to ensure that the methodology that was studied in parallel midbody region in the previous projects is applicable to the shaped regions of the hull. The two main differences between the current analysis and the previous work are the higher ice load at the bow, and the shaped hull geometry. Due to shaped hull, framing members are not perpendicular to shell, and this may introduce additional failure modes.

Basic analysis methodology and modelling techniques were studied and established in HULLFEM I and analyzed with example dry cargo vessels [1]. In HULLFEM II, a wide array of additional ship types and structural arrangements were analyzed to cover all typical vessels that operate on the Baltic Sea [2].

Using the knowledge basis from these three projects, draft rules are written for the use of direct calculations methods for the FSICR. The rule draft has been presented to Classification societies for commenting and updated and refined based on the comments received.

# 2 EXAMPLE VESSEL

## 2.1 EXAMPLE VESSEL FOR THE BOW MODEL

It was established in HULLFEM II that the proposed methodology works for a wide array of vessel types and structural configurations, on parallel midbody region [2]. The main question for this project is to study if the method is similarly applicable for a bow region. It is assumed that in case the method works for bow and midbody, it is applicable to stern, and separate analysis of a stern is not done.

Modeling and analyzing a bow is much more work intensive than parallel midbody, as structural elements cannot be simply copied from frame to frame. Therefore, only one bow was modeled and analyzed. The analyzed vessel was chosen to be the medium sized general cargo / dry cargo vessel from HULLFEM I & II, as those are the most common vessel type on the Baltic Sea [1]. Ice class was chosen as 1A.

Dry cargo vessels typically have open cross-section, double hull and one or several holds for carrying diverse types of cargo either in bulk or as packaged goods. Example of a typical general cargo / dry cargo vessel is shown in Figure 1. Main dimensions are shown in Table 1.


Figure 1 Typical Baltic Sea general cargo vessel (photo Suomen kuvitettu laivaluettelo 2021).

The same bow is directly applicable for the medium sized bulk carrier of HULLFEM II, due to similar main dimensions. While these vessels have different structural configuration on the midbody part, the bow configuration for both is similar. Similarly, the analyzed example bow could be applied to a container vessel, or with a slight modification of main dimensions, to the small LNG tanker of HULLFEM II.

Table 1 Main dimensions of the medium general cargo / dry cargo vessel.

| | | | |
|---|---|---|---|
| **FSICR** | **1A** | | *Ice class* |
| **$L_{oa}$** | 121 | m | *Length, overall* |
| **$L_{bp}$** | 115 | m | *Length, rule* |
| **B** | 20.3 | m | *Breadth* |
| **D** | 10.7 | m | *Depth* |
| **T** | 7.4 | m | *Draught* |
| **Δ** | 14200 | t | *Displacement* |
| **$C_b$** | 0.80 | | *Block coefficient* |
| **v** | 12 | kn | *Service speed* |
| **P** | 4000 | kW | *Shaft power* |

The hull shape for the bow was chosen to represent a typical modern EEDI (Energy Efficiency Design Index) bow that is mainly optimized for energy efficiency in open water, but with a shape that provides reasonable performance in ice as well. The hull shape is based on a vessel concept that Aker Arctic had designed couple of years ago. The parent bow was scaled slightly to match the main dimensions of the example vessel. Overall, it represents a very typical solution for moderate Baltic Sea conditions. The bow shape is shown in Figure 2.

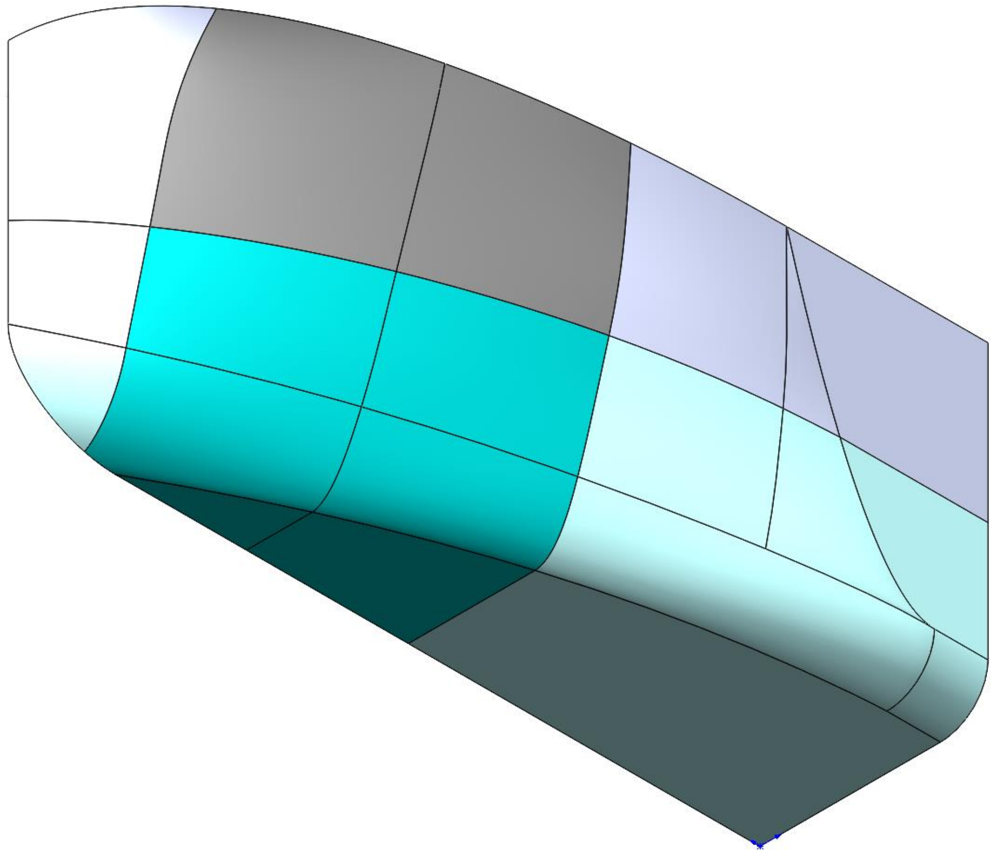

Figure 2 Bow shape of the example vessel. The modeled region is marked with darker color.

Similar to the previous study, the scantlings have been calculated to fulfill the open water Classification rules, and in general chosen to be reasonable and typical for the vessel type in question, to represent a typical design as closely as possible. The calculation for open water scantlings was done with Lloyd's Register RulesCalc 2018.

For ice class, scantlings were chosen to be lowest possible that fulfill the requirements of the current FSICR [3], as explained in more detail in the following chapter.

The example vessel was designed using HT-36 grade steel, as that is a relatively typical material in current shipbuilding.

Two alternative structural configurations were analyzed to cover cases with odd and even number of stringers. The aim was to ensure the applicability of the new rules for both cases and to ensure that results are not specific to span of web frames. First, the main bow model was done with an even number of stringers, as that was seen as the most typical structural configuration for the vessel in question. Then, the alternative model was made where the lower deck was moved one stringer spacing down, to obtain a model with odd number of stringers and longer web frame span, which results in one stringer at the midspan of the web frame.

The structure of the example bow is shown in Appendix A.

## 2.2 ADDITIONAL STUDIES

### 2.2.1 REANALYSIS OF WEB FRAMES FOR SINGLE SKIN VESSELS

In addition to the bow models, the midships of the medium LNG tanker and medium bulk carrier from HULLFEM II [2] were modified and reanalyzed. The HULLFEM II web frames were matched as closely as possible to both section modulus and shear area requirements of the current rules. This drove the web thicknesses to rather low values, which resulted in lot of web buckling related failures at loads where the web frames were otherwise not close to limits.

To more accurately reflect the capacity of current fleet and typical designs, the web frame profiles were changed from girder height of slightly above 600 mm and web thickness of 8 mm to girder height of 500 mm and web thickness of 10 mm. Instead of web height, the flange thickness was used as adjustment to tailor section modulus to rule minimum limit. This resulted in additional shear capacity over the rule minimum but reflects more accurately a typical design and reduced premature buckling failures.

The midship sections for the reanalyzed vessels are shown in Appendix C.

### 2.2.2 LOAD CASES FOR DECKS

In Class Society workshop, question was raised about applicable load cases for decks and bulkheads when those are used in lieu of a frame, stringer or web frame. For a bulkhead, the applicable load case is same as for a web frame, based on the previous experience. For decks, several different load cases were analyzed both with the example bow, and the RoPax vessel from HULLFEM II [2], to find the most onerous load case.

### 2.2.3 IDEALIZATION OF CUTOUTS

In Class Society comments, question arose about the idealization of ignoring the frame cutout in the mesh, as shown in Figure 3. To test the error caused by the idealization, a test case was run to compare the difference. The test was done with the medium bulk carrier with ice class IA and transverse framing with spacing of 400 mm. In the previous study [2], the load to cause the allowed 8 mm permanent deformation on a frame was 280.1 %. The model was modified to include frame cutout as shown in Figure 4 and analysis was rerun.

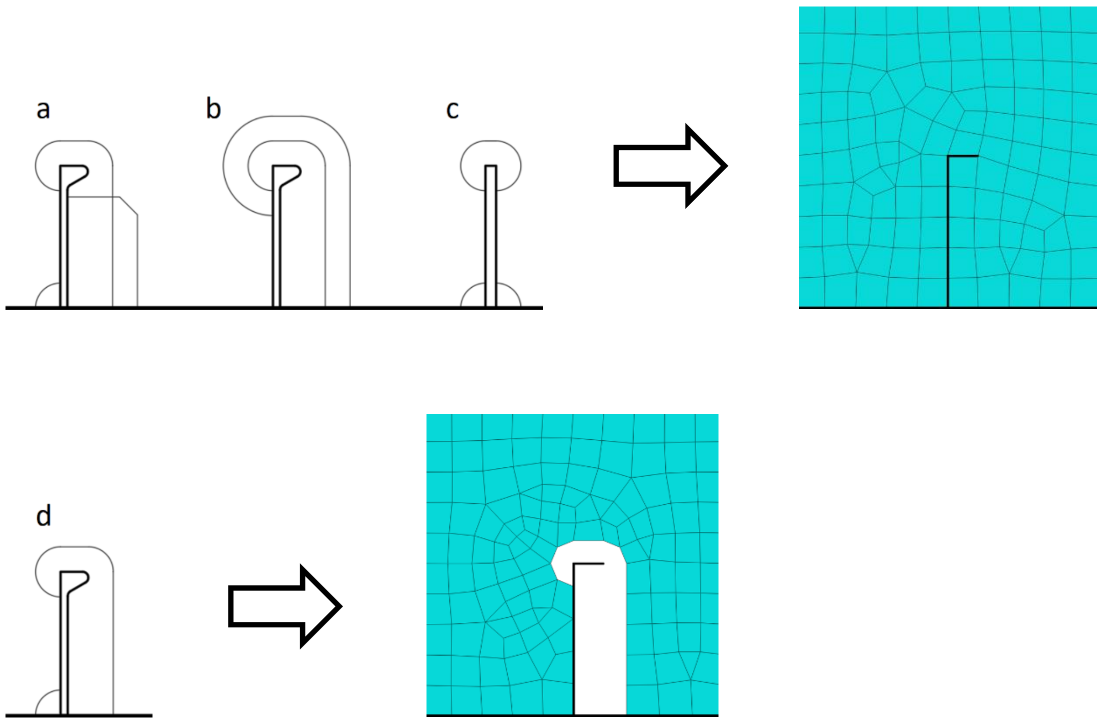


Figure 3 Modelling of cutouts for ice frames with cutout and lug (a), watertight collar (b), web directly welded to crossing member on both sides (c) and cutout connected to crossing member only on one side (d).

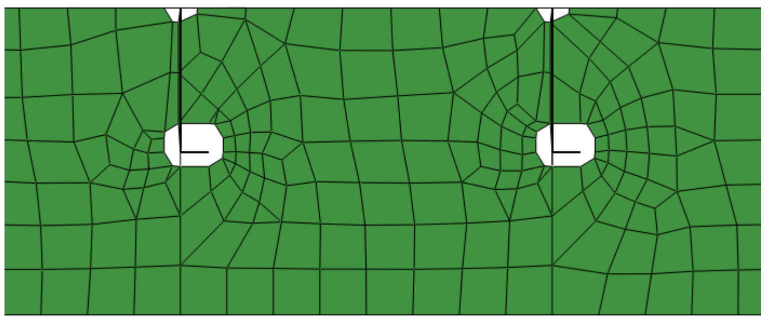

Figure 4 Mesh of the test model with cutouts modeled.

# 3 ANALYSIS METHOD

The methodology follows principles established in the first and second parts of the HULLFEM project [1] [2]. For more detailed information and background for choosing these methods, the reader is referred to those reports. For clarity, the used methods are summarized here.

## 3.1 FINITE ELEMENT MODEL

### 3.1.1 MODELING

The vessel was modeled and meshed in NAPA Designer. The mesh was then exported to Abaqus/CAE. Loads, boundary conditions, etc. were applied in Abaqus/CAE. The model was analyzed using Abaqus/Standard, and postprocessed in Abaqus/Viewer.

Model extents were taken as half ship, i.e. from centerline to side shell on one side, from baseline to strength deck, and six web frame spacings. Six web frame spacings was chosen because that provides at minimum two web frame spacings between the load and the boundary condition, preventing boundary effects from affecting the results with the dimensions of the example vessels. This model size was found to be the smallest suitable, based on earlier study [1].

Model and shell thicknesses can be seen in Figure 5, Figure 6, Figure 7 and Figure 8.

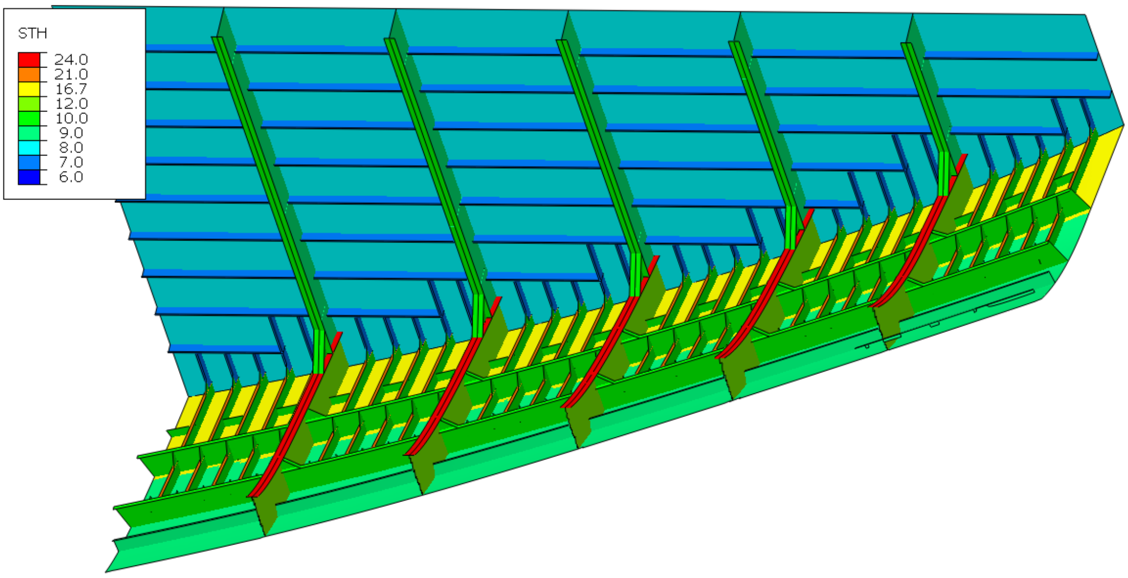


Figure 5 Shell element thicknesses, below lower deck.

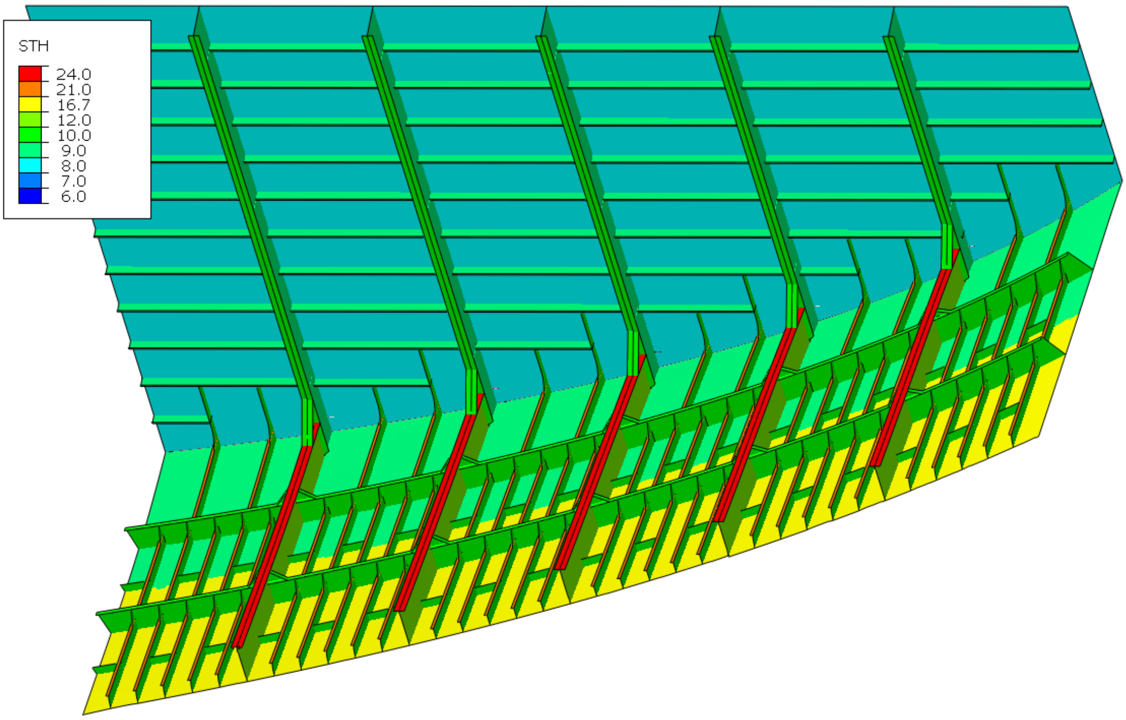


Figure 6 Shell element thicknesses, below main deck.

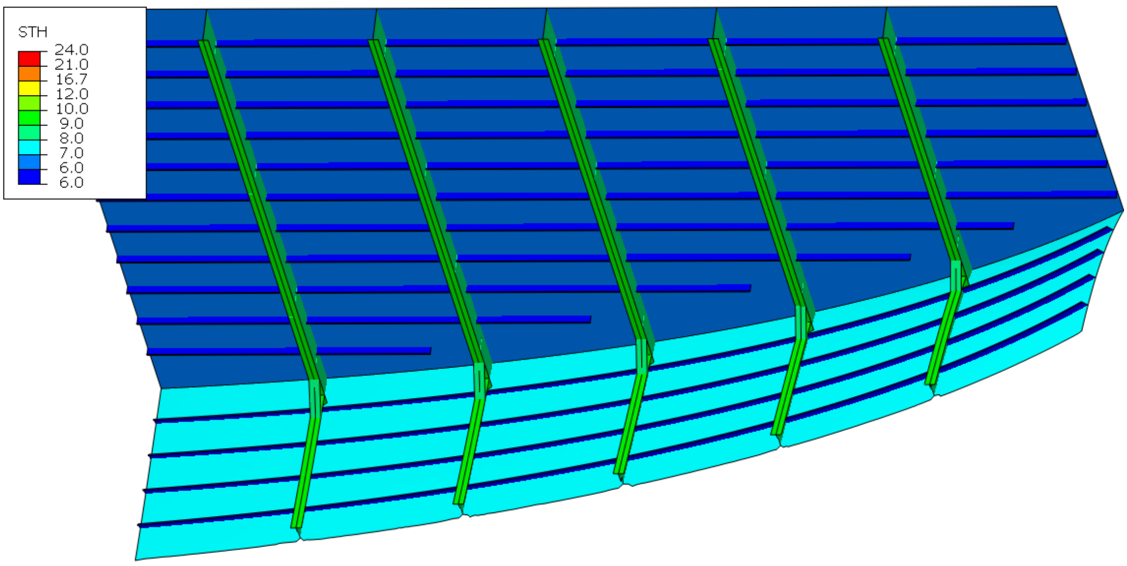


Figure 7 Shell element thicknesses, below forecastle deck.

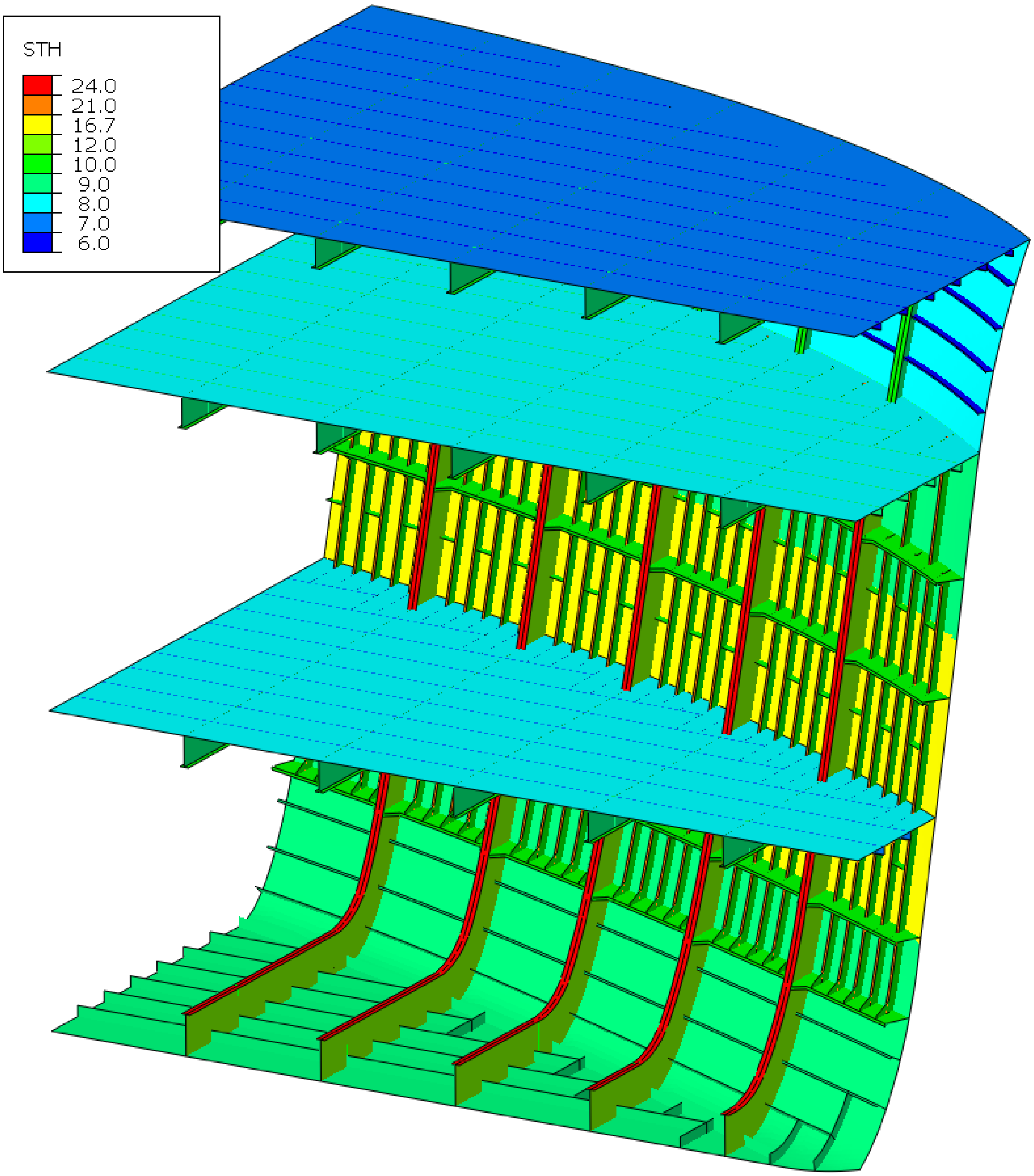


Figure 8 Shell element thicknesses, overview.

### 3.1.2 MESHING

Models were made fully with linear shell elements. Bulb profiles were modeled as equivalent L-profiles. In Abaqus documentation, element types S4R and S3R, which are quadrilateral (4-node) and triangular (3-node) general- purpose shell elements with reduced integration, hourglass control, and finite strain, are recommended for this type of analysis and these element types were used in this study [4].

As the model is made with shell element, the bulb profiles were converted to equivalent L-profiles. Like previous studies, this was done based on the CSR formula [1]. As discussed in the previous study [2] and illustrated in Figure 9, the web height of the equivalent L-profile was increased by half of plate thickness of equivalent flange and shell plate, to compensate for the thickness of shell plate being centered on the moulded hull surface in the model, instead of being completely outside. While this introduces minor error in shear capacity of the frame profile, and very minor error in section modulus due to excess web height, testing proved that this idealization offers much more exact representation of the actual capacity of the frame. [2]

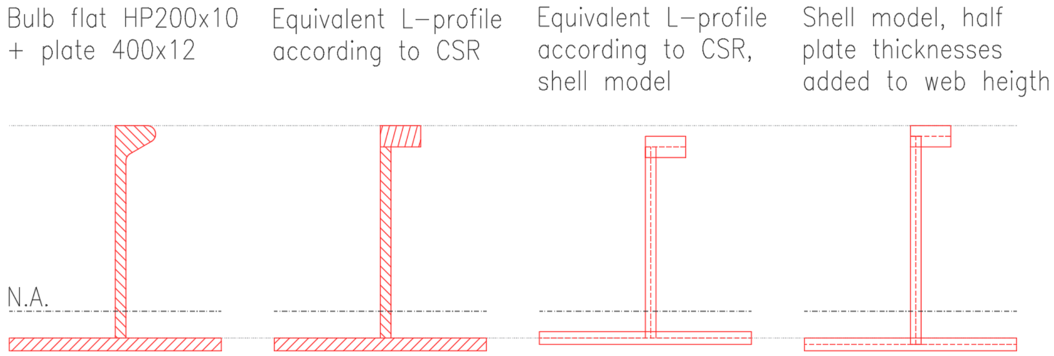


Figure 9 Idealization of bulb flat as L-profile. For clarity, effective plate width is halved in figure.

Mesh density was taken as minimum 8 elements on shell plate between each stiffener, and as minimum 3, preferably 4, elements across stiffener web. These mesh density guidelines follow the recommendations of Classification Societies for similar type of analysis [5], [6] and [7], and were found to work well on the previous parts of the HULLFEM project [1], [2].

Mesh for the bow model is shown in Figure 10 and Figure 11.

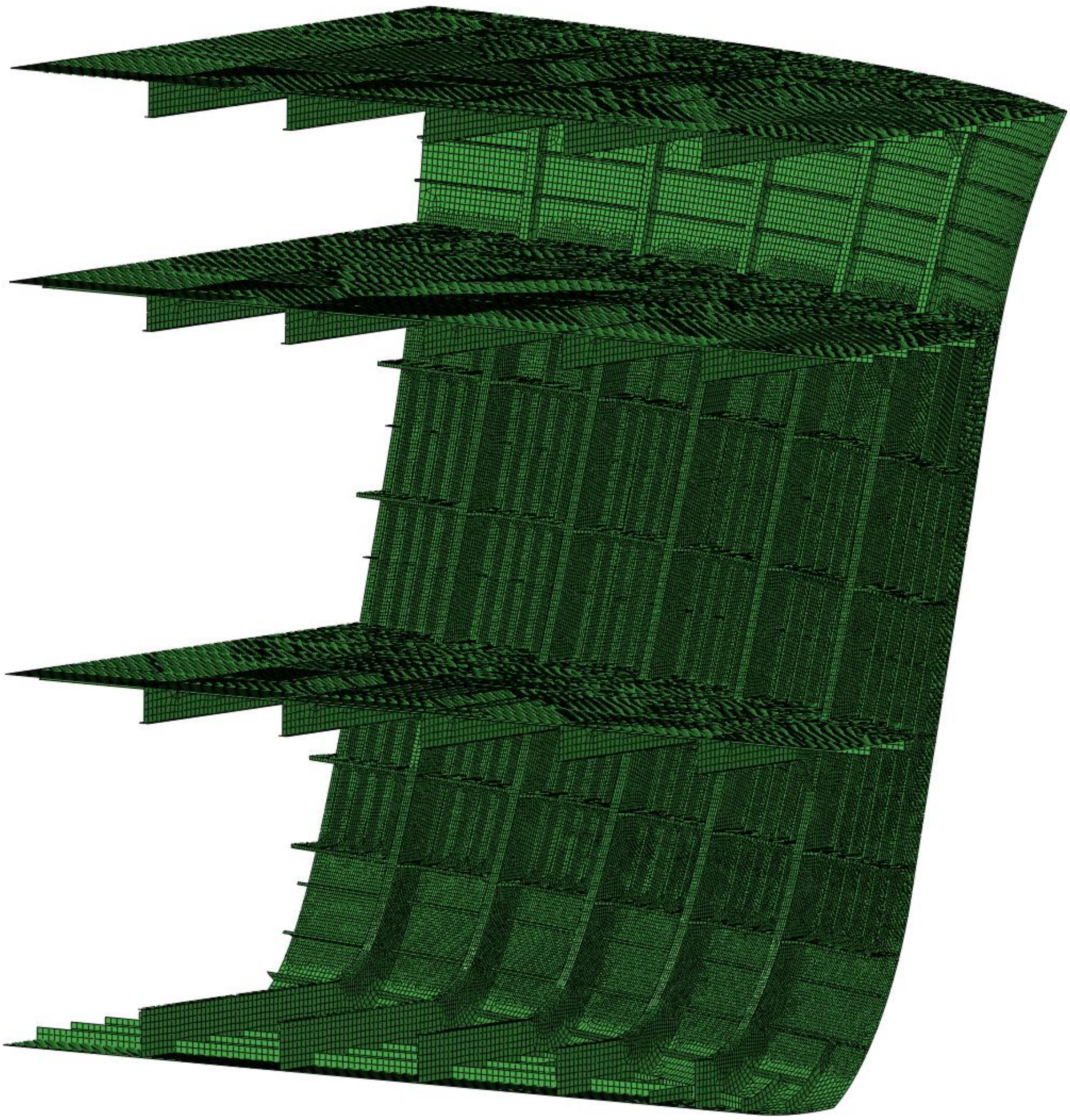

Figure 10 Overview of mesh.

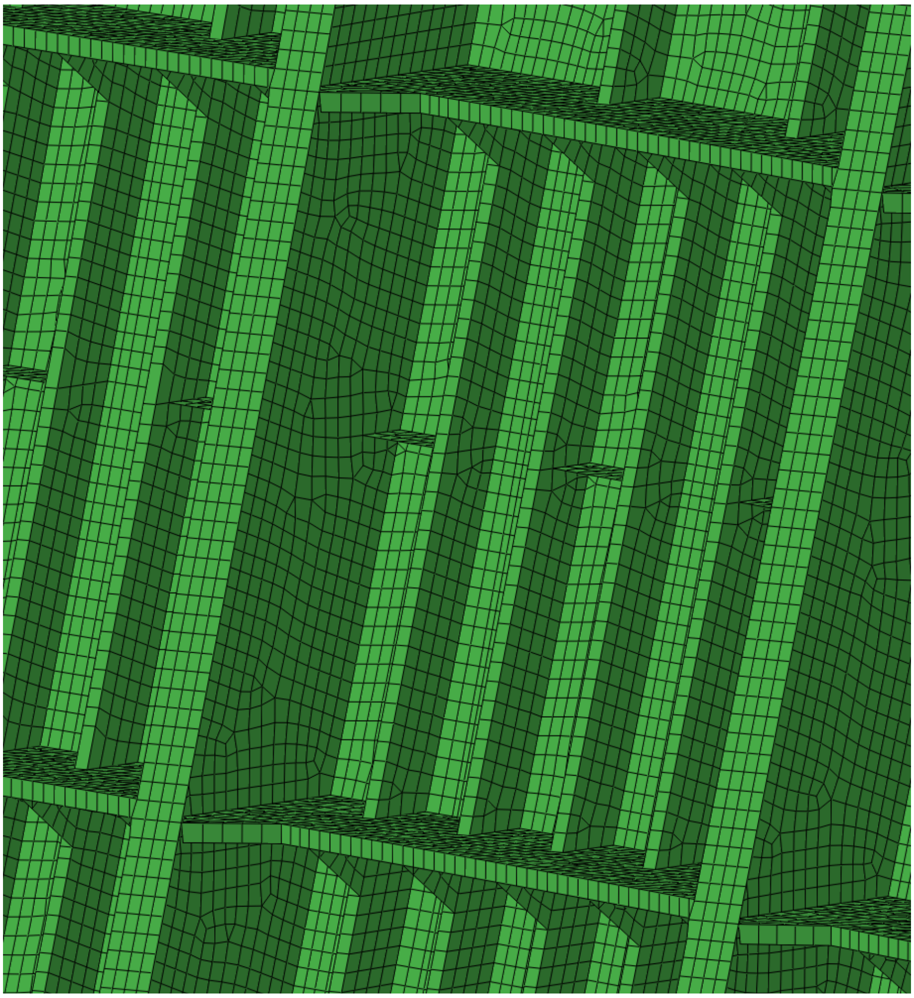

Figure 11 Detail of mesh, ice frames between stringers and web frames.

### 3.1.3 MATERIAL MODEL

Material was modeled as bilinear elastic-plastic with plastic modulus (tangent modulus) $E_t$ of 1000 MPa, as this model is widely used, see for example [5], [6] and [8]. In the previous study [1], it was found to produce very similar results to more complicated material models found in [6] and [7] at the relevant deformations [1]. As per Abaqus convention, all stresses and strains are taken as true stress and true strain. The material parameters for HT-36 grade steel are shown in Table 2.

Table 2 Material parameters for HT-36 steel.

| Steel grade | Yield | Ultimate | | Elongation | Abaqus material model | | | |
|---|---|---|---|---|---|---|---|---|
| | | | | | Yield | | Ultimate | |
| | | min | max | $A_{50}$ | $\sigma$ | $\varepsilon_{pl}$ | $\sigma$ | $\varepsilon_{pl}$ |
| HT-36 | 355 | 490 | 620 | 21 % | 355.6 | 0.0 | 681.6 | 0.1873 |

### 3.1.4 LOAD

Load is applied as a rectangular patch with evenly distributed pressure, similar to the previous studies [1], [2]. The load patch dimensions are taken directly from the Finnish-

Swedish Ice Class Rules [3], as that was found to be a reasonable approach in the previous study [1]. The load patch lengths for various structural elements are shown in Table 3.

Table 3 Load patch lengths for various structures [3].

| Structure | Type of framing | $l_a$ [m] |
|---|---|---|
| Shell | Transverse | Frame spacing |
| | Longitudinal | 1.7×Frame spacing |
| Frames | Transverse | Frame spacing |
| | Longitudinal | Span of frame |
| Ice Stringer | | Span of stringer |
| Web frame | | 2×Web frame spacing |

The element mesh does not always align perfectly with the load patch. The applied load patch area was taken always as the closest possible match to load patch dimensions from the rules. Then, the pressure was adjusted to obtain equivalent force:

$$p_{FEM} = p_{Rules} \frac{A_{Rules}}{A_{FEM}}$$

The exact load areas, locations, patch sizes and pressures for each vessel and load case are shown in Table 4 and Table 5. The error in load patch dimensions is less than half of element size, which was 50 mm, meaning that the error in each load patch dimension was about 25 mm or less. Compared to typical load patch height of 220 to 350 mm and width of 400 to 4800 mm, the error can be considered small.

Table 4 Load patch locations, dimensions and loads for the bow model.

| | location | | Rules | | | | | Model | |
|---|---|---|---|---|---|---|---|---|---|
| | X | Z | p | l | h | A | F | A | p |
| | mm | mm | MPa | mm | mm | cm2 | kN | cm2 | MPa |
| Shell 1 | 7800 | 6100 | 2.554 | 433 | 300 | 1299 | 332 | 1380 | 2.404 |
| Shell 2 | 8200 | 5650 | 2.554 | 433 | 300 | 1299 | 332 | 1265 | 2.623 |
| Shell 3 | 8200 | 6550 | 2.554 | 433 | 300 | 1299 | 332 | 1324 | 2.506 |
| Frame 1 | 8400 | 6000 | 2.554 | 433 | 300 | 1299 | 332 | 1286 | 2.580 |
| Frame 2 | 8400 | 4200 | 2.554 | 433 | 300 | 1299 | 332 | 1370 | 2.421 |
| Frame 3 | 8000 | 6000 | 2.554 | 433 | 300 | 1299 | 332 | 1323 | 2.507 |
| Stringer 1 | 8400 | 7000 | 1.223 | 2615 | 300 | 7845 | 959 | 7988 | 1.201 |
| Stringer 2 | 8400 | 3400 | 1.223 | 2615 | 300 | 7845 | 959 | 8309 | 1.155 |
| Webframe 1 | 7200 | 7900 | 0.894 | 5173 | 300 | 15519 | 1387 | 15547 | 0.892 |
| Webframe 2 | 7200 | 7000 | 0.894 | 5173 | 300 | 15519 | 1387 | 15550 | 0.892 |
| Webframe 3 | 7200 | 3400 | 0.894 | 5173 | 300 | 15519 | 1387 | 16255 | 0.854 |
| Deck 1 | 7200 | 5200 | 0.894 | 5173 | 300 | 15519 | 1387 | 15907 | 0.872 |
| Deck 2 | 8400 | 5200 | 1.223 | 2615 | 300 | 7845 | 959 | 8185 | 1.172 |

Table 5 Load patch locations, dimensions and loads for the bow model with alternative structural configuration.

| | location | | Rules | | | | | Model | |
|---|---|---|---|---|---|---|---|---|---|
| | X | Z | p | l | h | A | F | A | p |
| | mm | mm | MPa | mm | mm | cm2 | kN | cm2 | MPa |
| Stringer 3 | 8400 | 7000 | 1.223 | 2615 | 300 | 7845 | 959 | 7989 | 1.201 |
| Webframe 4 | 7200 | 7000 | 0.894 | 5173 | 300 | 15519 | 1387 | 15542 | 0.893 |
| Webframe 5 | 7200 | 5200 | 0.894 | 5173 | 300 | 15519 | 1387 | 15942 | 0.870 |

In this study, load was applied to find the plastic capacities as defined in 3.2.3 for shell plate, frame, stringer (for transversally framed vessels) and web frames. In addition, shell analysis was run up to permanent deformation of 5 % of frame spacing as discussed in 3.2.4, as that was found in the previous study to be the upper limit of ice related damages on the Baltic Sea [1], and can be therefore thought to be the absolute maximum for the load that the structure must be able to withstand without major failure.

For each structural member, most onerous location(s) for the load patch were selected, following the findings from the previous study [1]. In case the most onerous location was not obvious, several locations were used to find the most onerous one. The analyzed load patch locations are shown in Figure 12, Figure 13 and Figure 14. For clarity, the load patch locations for the main model are divided into two figures.

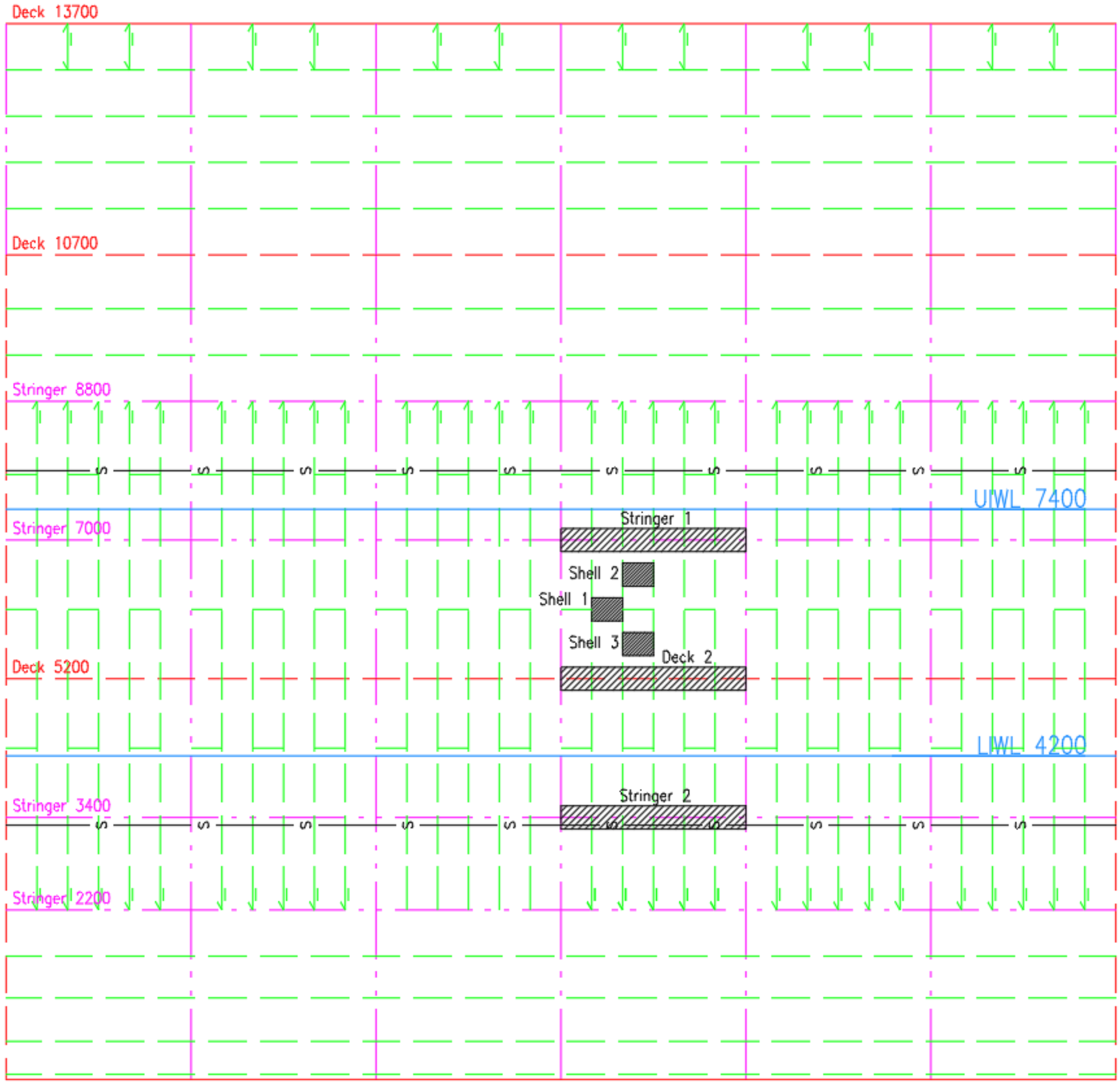


Figure 12 Load patch locations for the bow, shell and stringers.

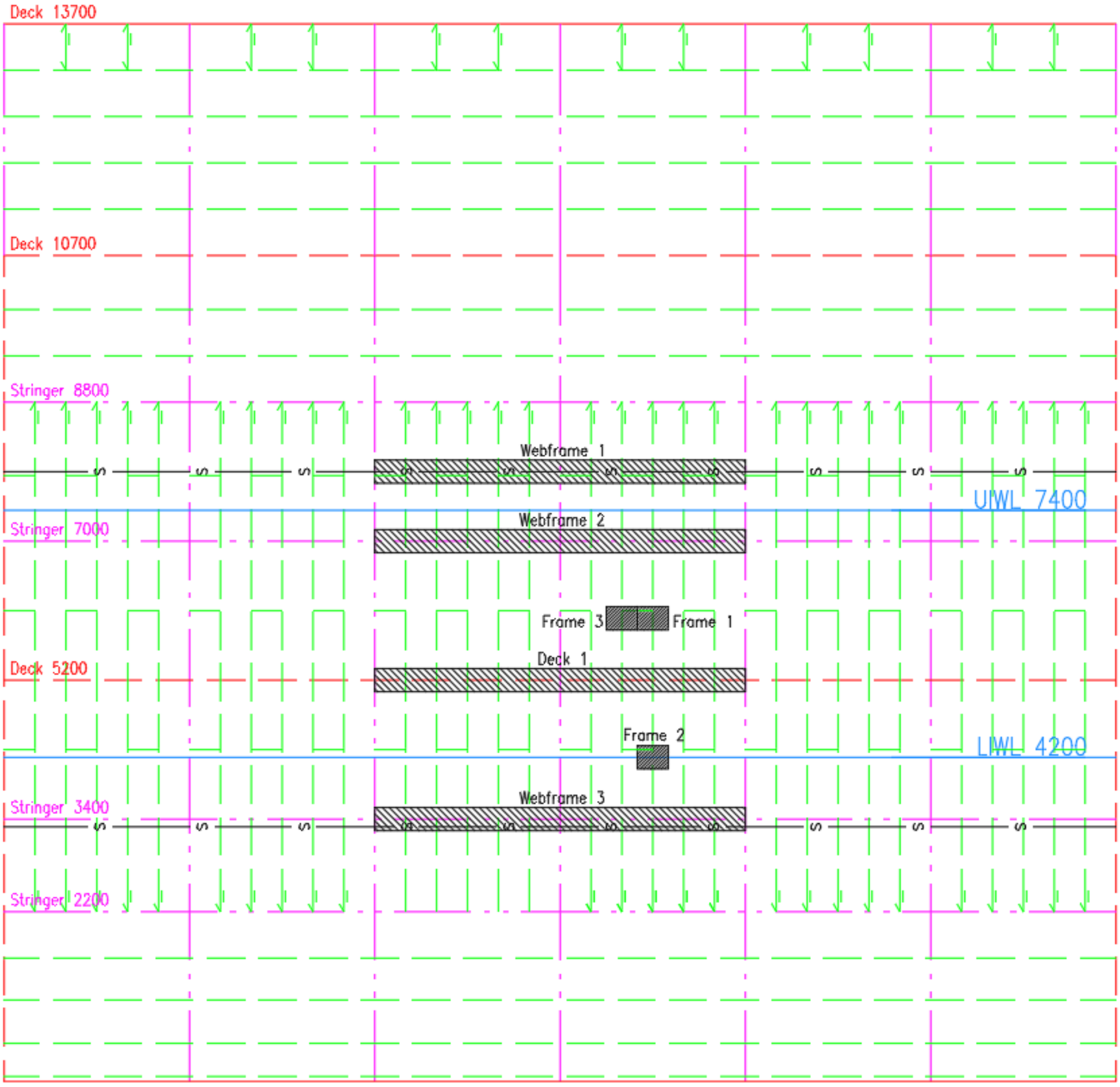


Figure 13 Load patch locations for the bow, frames and web frames.

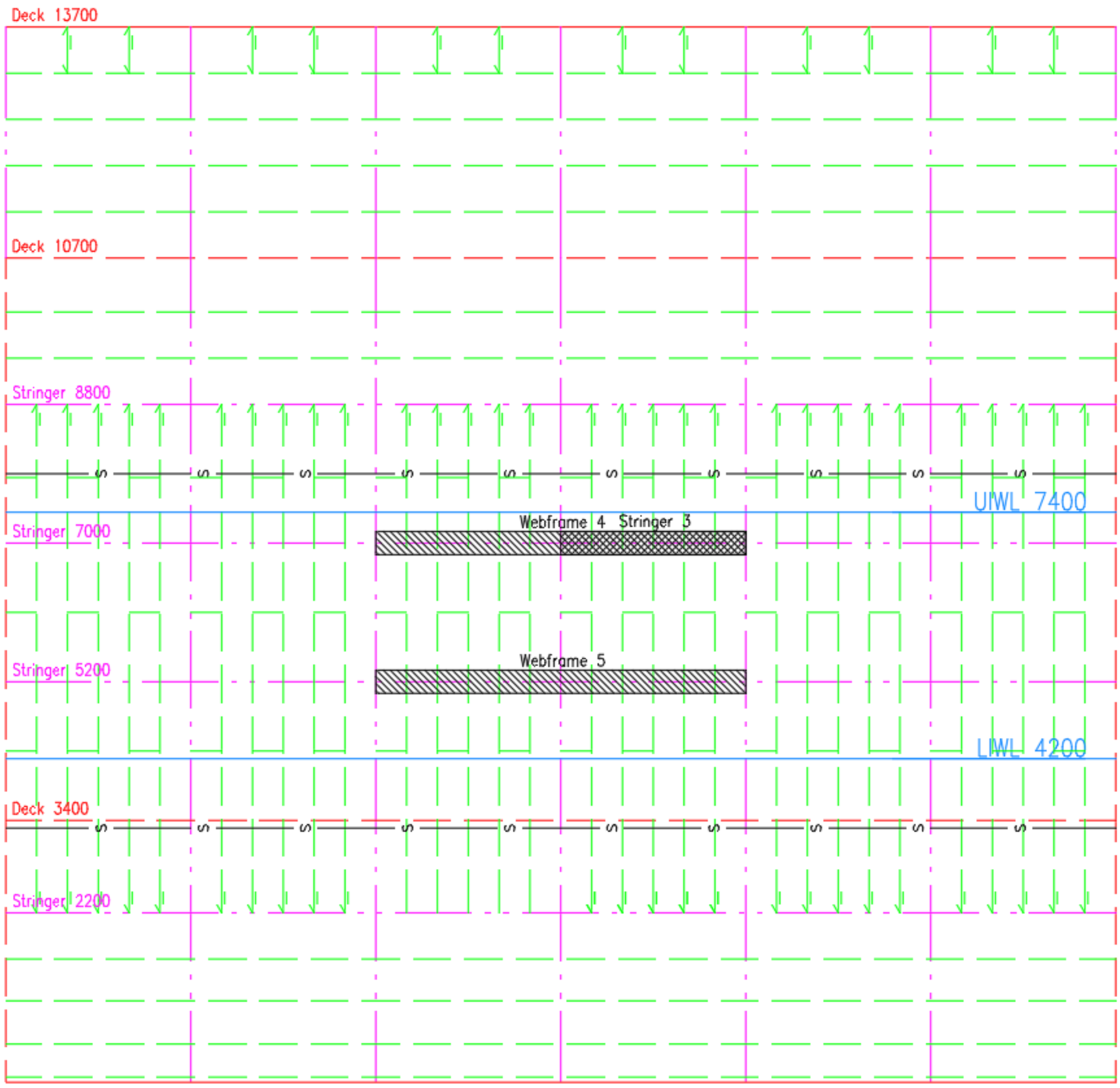


Figure 14 Load patch locations for the bow with alternative structural configuration.

### 3.1.5 BOUNDARY CONDITIONS

Boundary conditions were applied using the practices that were found to work well on the previous studies [1], [2]. Boundary conditions were applied to the model edges where the structure continues. At centerline and at model ends, pinned boundary conditions were applied.

An example of loading and boundary conditions is shown in Figure 15. Boundary condition marked in orange refers to a pinned boundary. Applied pressure load is shown in magenta.

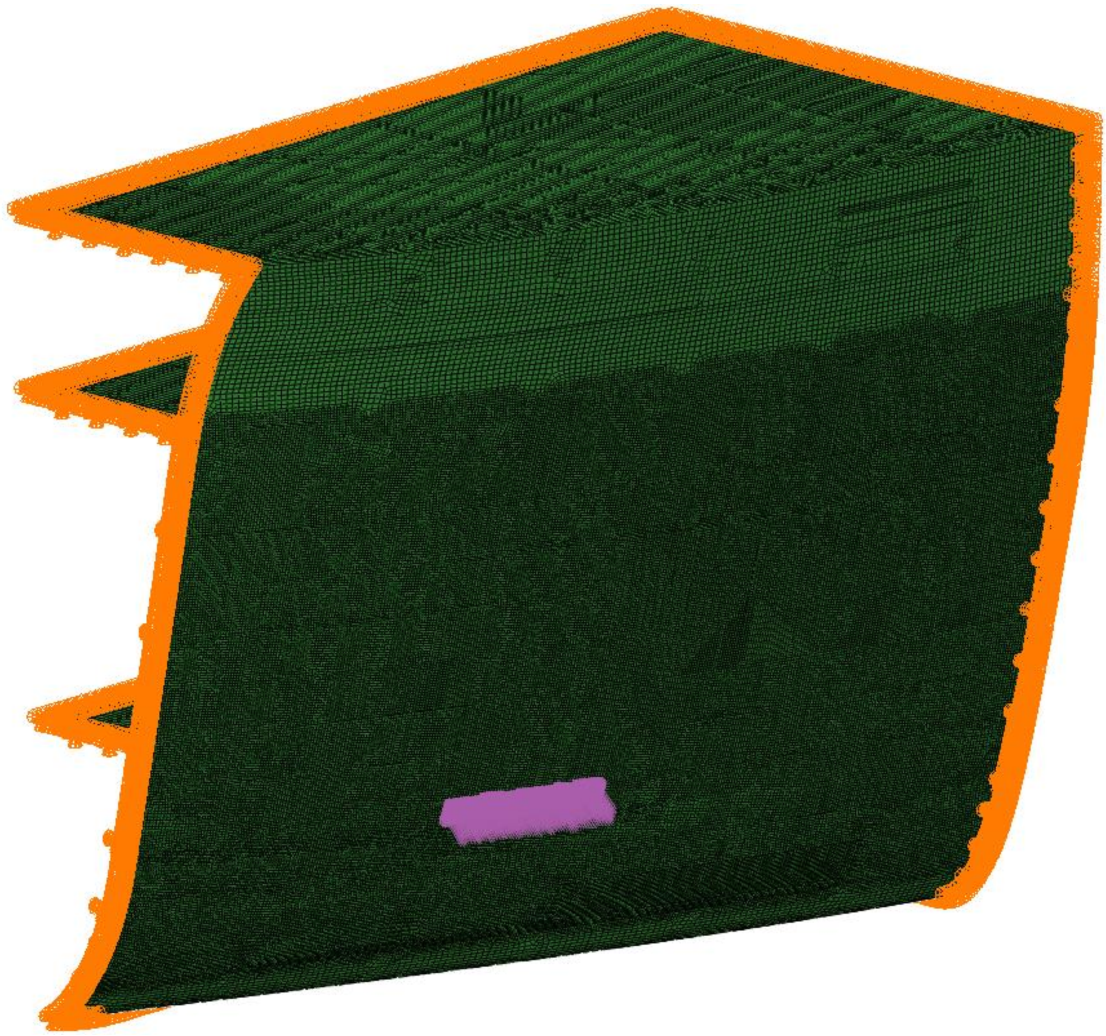

Figure 15 Boundary conditions and a typical load patch on the model.

## 3.2 ANALYSIS

### 3.2.1 SOLUTION AND INCREMENTATION

The analysis is made with implicit solver.

Incrementation is set automatic, so that Abaqus solver can vary the load increment to find optimum for obtaining a stable solution with minimum computational effort. Selecting suitable maximum load increment is a balance between acceptable accuracy and computational cost. In the previous study, several options were tested [2].

For cases where the response was governed by a plastic hinge type mechanisms or very gradual buckling, it was found that Abaqus automatic incrementation works as intended and provides accurate results. Thus, automatic incrementation was used for all cases where the iteration converged easily, and no special reason was found for further investigation. [2]

The step size for the automatic incrementation varies with the load. For some of the more complicated cases, where the response is governed by a rapid buckling failure, it was found that this variation in increment affected the results. Thus, for these cases, it was found necessary to control the maximum step size, to ensure that onset of rapid buckling was captured accurately by incrementing the load with sufficiently small steps close to the load causing buckling. The maximum load increment values shown in Table 6 were found to offer reasonable balance between accuracy and computational cost for these problems and were used when found necessary. In all cases, Abaqus Solver was allowed to use smaller load increments when necessary to find a stable and accurate solution. [2]

Table 6 Maximum load increments for the solver for cases including rapid buckling, as percentage of total load.

| Load | Maximum increment |
|---|---:|
| 0 % - 60 % | 10 % |
| 60 % -75 % | 2 % |
| 75 % - 85 % | 1 % |
| 85 % - 92.5 % | 0.5 % |
| 92.5 % - 100 % | 0.25 % |

### 3.2.2 ITERATION

When calculating the permanent deformation of the structure after being subjected to a known load, the permanent deformation can be obtained directly, by first loading and then releasing the load on the structure in FE. This is the method recommended when analyzing a structure according to the proposed new rules.

However, for calculating the capacity of a known structure at a known deformation, the calculation cannot be performed directly. Instead, initial guess of the load is made, the load is applied and released, the deformation is calculated, and then the load is adjusted iteratively to find the load corresponding to the target deformation. In practice, this was achieved by programming a python script that ran Abaqus analysis iteratively and adjusted the load until the load to cause the desired permanent deformation was found.

### 3.2.3 DEFINITION OF CAPACITY LIMIT FOR PERMANENT DEFORMATION ANALYSIS

The goal of the permanent deformation analysis is to ensure that the permanent deformations in normal service do not exceed newbuilding tolerances. In other words, the aim is to ensure that in normal service, if any denting of structure occurs, it is sufficiently small that it does not require repair and does not affect the capability of the structure to carry other loads (open water, hull girder bending, cargo, etc.). In principle, as long as possible deformations from ice loads remain below newbuilding tolerance, it is not possible to determine afterwards if dent has been caused by an ice load or has been there since the vessel has been built. [8]

The plastic capacity of the structure is defined as the load at which the permanent deformation of the structure exceeds the limits of IACS newbuilding quality standard [9]. For the structures in question, this limit is most typically 8 mm or 0.3 % of span for framing members. Based on the discussion of the Classification Society Workshop, the limits of the previous study [1] were further simplified to requiring that the total permanent deformation of all members shall not exceed 8 mm. The deformation was taken as total deformation magnitude, i.e.

$$\delta = \sqrt{\delta_x^2 + \delta_y^2 + \delta_z^2}$$

In the previous studies, one limit state for the structure was that von Mises stress was not allowed exceed the minimum ultimate strength of the material when the design load is applied [1], [2]. This limit was added as an additional safety, to try and ensure that rupture would be prevented.

Stress is directly dependent on strain, which is dependent on meshing and thus not as robust measure as deformation [8]. In essence, the limit for allowed plastic strain (or stress) should depend on mesh [10]. The two recommended criteria would be either to limit the allowed plastic strain to a very small value, such as 0.02 (2 %) as proposed in [10], or to do a calibration study for the particular mesh [10].

Based on the results of the analyses of the example vessels, the smaller limit of 2 % plastic strain would be limiting for some cases, before the permanent deformation limit is reached. However, when the mesh calibration study was done for these cases to obtain the more accurate limit, it became very clear that the calculated plastic strains were well below the allowable values for the particular mesh. With the used meshes, the allowable plastic strain limits were around 0.13…0.16. Based on the results of the example vessels, it is clear that the strain (or stress) limit is never even close to being the governing limit, and thus not worth the required additional analysis effort, especially including the separate calibration study required. Therefore, the stress limit is removed from the criteria, as it is clear that the permanent deformation criteria is sufficient.

### 3.2.4 DEFINITION OF CAPACITY LIMIT FOR ULTIMATE STRENGTH ANALYSIS

In addition to permanent deformation analysis, ultimate strength analysis is included in the rule proposal. The goal of the ultimate strength analysis is to ensure that the structure has sufficient plastic reserve so that typical maximum ice loads encountered on the Baltic Sea do not lead to loss of load-carrying capacity resulting in major damage. In essence, this means that the overload capacity that was previously ensured by strict requirements for the structural arrangement is now ensured by the ultimate strength analysis.

As discussed in HULLFEM II, the earlier damage studies [11], [12] showed that for ice damages on vessels designed to strength level comparable to the requirements of the current rules (i.e. vessels designed to FSICR of 1985 or later), the typical maximum deformation is shell deformation of 5 % of frame spacing [2]. Thus, this can be considered to represent the typical upper limit of the accidental ice loads in the Baltic Sea merchant vessel fleet. Therefore, all example vessels have been analyzed to find the load that would cause this level of permanent deformation. That defines the maximum load that the structure should survive without catastrophic failure, such as major buckling, collapse or rupture leading to loss of load-carrying capacity or watertight integrity. The intent is that at this ultimate / accidental load, the structure may have permanent deformations that require repair at next drydocking, but that the structure should retain safe behavior and not require emergency repairs. Namely, the structure should behave in such way that load-carrying capacity is retained after the ultimate load has passed.

The way to identify loss of load-carrying capacity is to observe the slope of the load-deformation curve. As long as there is a continuously positive slope on the load-deformation curve, a finite increase in load will lead to a finite increase in permanent deformation, i.e. structure is able to carry and distribute the load effectively, even if it is permanently deformed. If there is (even locally) a zero or negative slope on the load-deformation curve, it means that at that point the structure has lost load-carrying capacity and a small increase in load may lead to a large increase in permanent deformation. In other words, the structure has failed, at least in local sense, and the ability of the structure to carry any further load is compromised. Typically, this can happen because of buckling or tripping of such nature that post-buckling capacity is less than pre-buckling capacity, or by complete plasticization of structure.

This is unsafe and therefore undesired response for ice-strengthened structure. Therefore, the rule proposal prohibits this kind of response at loads up to the upper limit of accidental ice loads observed on the Baltic Sea, i.e. the load that causes on shell plating a permanent deformation of 5% of frame spacing. In practice, this is done by requiring the load-deformation curve to have a positive slope at all points from zero to the ultimate ice load, which is defined as the ice load that causes on shell plating a permanent deformation of 5% of frame spacing.

# 4 RESULTS

All loads in this chapter are presented as percentage of the rule design ice load, unless otherwise noted.

## 4.1 BOW MODEL

The load at which each structural element reached the permanent deformation limits defined in 3.2.3 are shown in Table 7 and Table 8. As the models are otherwise identical, and the only difference is the arrangement of the primary structures, the results for shell and frames are not repeated for the model with the alternative primary structure, as they would be identical within calculation accuracy.

The results for the bow model are compared to the results for the midbody of the same vessel in Table 9. As can be seen, the results are generally well aligned, and variation is within the variation observed between different ships in HULLFEM II [2]. This means that there is no definite trend between models of parallel midbody and models of shaped bow region, meaning that the results from one hull region can be generalized to be applicable for all hull regions.

For shell plate and frames, the model behaves in expected way and plastic behavior follows classical plastic hinge mechanism. No instability was observed in the framing. The results are in fair agreement with the previous analysis work of HULLFEM II [2]. The tripping brackets are adequate to prevent any instability that might arise from the framing being not perpendicular to the shell. It was also observed that tripping brackets do not distribute the load to adjacent frame that effectively, and the frame under the load carries most of the load.

For stringers, no instability was observed, and plastic behavior follows classical plastic hinge mechanism. As usual, brackets for frames provide efficient buckling support for the stringer web. For the alternative structure, stringers were governing case for the primaries. For the main model, limiting load case was web frame, but stringer was close to that. It is clear that for stringers, the design is driven by ice class. The results align well with the previous analysis work of HULLFEM II [2].

For web frames, the main mechanism was formation of plastic hinges. Additionally, web buckling of the deck girders supporting the web frames was observed. Notably, in the load case web frame 1, which was the governing load case for the primary structure of the main model, the load was applied at centre of the effective span, between stringers. It is clear that for web frames, the design is driven by ice class. The results align well with the previous analysis work of HULLFEM II [2].

More detailed results, load-deformation curves, displacement plots and stress plots for each load case are presented in Appendix B.

Table 7 Summary of the results for the bow.

| Load case | Load |
|---|---|
| Shell | 251.0 % |
| Frame | 286.2 % |
| Stringers | 387.6 % |
| Web frames | 376.8 % |
| Shell 5% | 341.4 % |

Table 8 Summary of the results for the bow with the alternative primary structure.

| Load case | Load |
|---|---|
| Stringers | 359.3 % |
| Web frames | 403.3 % |

Table 9 Comparison of bow and midbody of the 10 000 DWT IA dry cargo (double side) and bulk carrier (single side).

| Ship | Plastic capacity | | | |
|---|---|---|---|---|
| | Shell | Frame | Stringers | Web frames |
| IA midbody, double side | 291 % | 277 % | > 1000 % | 349 % |
| IA midbody, single side | 269 % | 280 % | 355 % | 485 % |
| IA bow, single side | 251 % | 286 % | 388 % | 377 % |
| IA bow, single side, alternative structur | 251 % | 286 % | 359 % | 403 % |

## 4.2 REANALYSIS OF HULLFEM II VESSELS WITH SINGLE SIDE

The load at which each structural element reached the permanent deformation limits defined in 3.2.3 are shown in Table 10. The original models analyzed in HULLFEM II had web frames with web thickness of 8 mm and web height around 600 mm, and both web frame shear area and section modulus were minimized to exactly pass the rule minimum requirements. The modified models had web frames with web thickness 10 mm, web height of 500 mm and flange dimensions chosen to minimize the section modulus to just pass the rule minimum requirements. The modified configuration is considered to be more representative of typical arrangement.

As can be seen from Table 10, the modification of using slightly thicker and lower web for the web frames increased the capacity of both stringers and web frames significantly, even though the nominal section modulus remained the same. The difference is due to the original webs failing prematurely in buckling. The results show that web frame capacity of 425 % of rule design load is easily achievable with reasonably chosen scantlings and stiffening arrangements for all cases. Further, this example demonstrates the power of non-linear finite element method in determining not only the failure load, but also cause of the failure, which allows designers to improve the structure, often with much smaller weight impact than just adding thickness.

More detailed results, load-deformation curves, displacement plots and stress plots for each load case are presented in Appendixes D, E, F, G, H and I.

Table 10 Summary of the results for the single sided vessels of HULLFEM II with original and modified web frames.

| Ship | Stringers | | Web frames | |
|---|---|---|---|---|
| | Original | Modified | Original | Modified |
| Medium LNG tanker | 350 % | 372 % | 381 % | 477 % |
| Medium bulk carrier, T 400 | 344 % | 355 % | 465 % | 485 % |
| Medium bulk carrier, T 600 | 377 % | 385 % | 428 % | 521 % |
| Medium bulk carrier, T 800 | 391 % | 397 % | 424 % | 519 % |
| Medium bulk carrier, L 400 | - | - | 424 % | 440 % |
| Medium bulk carrier, L 600 | - | - | 397 % | 471 % |

## 4.3 LOAD PATCH SIZE AND LOCATION FOR DECKS

The load at which the deck reached the permanent deformation limits defined in 3.2.3 are shown in Table 11.

For all cases, model behaves as expected, and the decks fail by buckling. As the load patch is located at the deck height, most of the load is carried directly by the deck, and other structures are not close to capacity limits. Some local yielding is observed on shell plating and framing, but this is expected, given the high load levels involved. For the bow model, locating the shorter load patch centered on web frame was not studied, since results from the RoPax showed that this would clearly not be the governing load case.

As can be seen from Table 11, the governing load case for both models was a load patch with length of one web frame spacing, located between web frames. This is similar to stringers, meaning that when there is a deck in lieu of a stringer, the same load case as for stringer is applicable.

More detailed results, load-deformation curves, displacement plots and stress plots for each load case for the bow model are presented in Appendix B and for the RoPax in Appendix J.

Table 11 Summary of the results for the deck load cases.

| Model | Case | Load length | Location | Plastic capacity |
|---|---|---|---|---|
| RoPax | Deck 1 | 1 web spacing | Centered on web | 883.1 % |
| | Deck 2 | 2 web spacings | Centered on web | 735.5 % |
| | Deck 3 | 1 web spacing | Between webs | 585.6 % |
| Bow | Deck 1 | 2 web spacings | Centered on web | 775.6 % |
| | Deck 2 | 1 web spacing | Between webs | 586.8 % |

## 4.4 IDEALIZATION OF CUTOUTS

The maximum permanent deformation of frame after being loaded to a load of 280.1 % of rule load is shown in Table 12. As can be seen from the results, the effect of the cutouts on the frame capacity is minor, and the chosen idealization can be considered acceptable.

More detailed results, load-deformation curves, displacement plots and stress plots for each case are presented in Appendix K.

Table 12 Summary of the results for the cutout idealization test.

| Cutout modeling | Permanent deformation |
|---|---|
| Idealized | 8.000 mm |
| Real geometry | 7.557 mm |

## 4.5 RESULTS OF HULLFEM II AND III COLLECTED TOGETHER

The results of all example vessels are collected together in Table 13. For each vessel and structural element, the plastic capacity is ice pressure as percentage of the current rule design ice pressure that is required to reach the plastic limit states as defined in 3.2.3 and 3.2.4.

Table 13 All results of HULLFEM II and III collected together. Outliers marked with *grey*. For vessels reanalyzed in HULLFEM III, newer results shown.

| Ship | Displ. | Ice class | Framing | | | Plastic capacity | | | | |
|---|---|---|---|---|---|---|---|---|---|---|
| | | | Dir | Spc. | Side | Shell | Frame | Stringer | Web fr. | Shell 5% |
| Small dry cargo | 4960 | IA | T | 400 | Double | 287 % | 297 % | *> 900%* | 473 % | 399 % |
| Medium dry cargo, IC | 14100 | IC | L | 600 | Double | 363 % | 293 % | - | *832 %* | *732 %* |
| Medium dry cargo, IA | 14200 | IA | T | 400 | Double | 291 % | 277 % | *> 1000 %* | 349 % | 454 % |
| Medium dry cargo, IAsuper | 14360 | IAsup | T | 400 | Double | 276 % | 321 % | *745 %* | *568 %* | 414 % |
| Large dry cargo | 69930 | IA | L | 700 | Double | 311 % | 310 % | - | 439 % | 557 % |
| Medium LNG tanker | 9400 | IA | T | 400 | Single | 270 % | 266 % | 372 % | 477 % | 403 % |
| Large tanker | 132500 | IA | L | 800 | Double | 290 % | 287 % | - | 329 % | 541 % |
| Medium bulk carrier, T 400 | 14200 | IA | T | 400 | Single | 269 % | 280 % | 355 % | 485 % | 395 % |
| Medium bulk carrier, T 600 | 14200 | IA | T | 600 | Single | 197 % | 241 % | 385 % | 521 % | 391 % |
| Medium bulk carrier, T 800 | 14200 | IA | T | 800 | Single | 255 % | 239 % | 397 % | 519 % | 534 % |
| Medium bulk carrier, L 400 | 14200 | IA | L | 400 | Single | 309 % | 303 % | - | 440 % | 431 % |
| Medium bulk carrier, L 600 | 14200 | IA | L | 600 | Single | 238 % | 377 % | - | 471 % | 562 % |
| RoPax | 31605 | IAsup | T | 400 | Single | 243 % | 272 % | 403 % | 481 % | 342 % |
| Medium dry c. / bulker, Bow | 14200 | IA | T | 400 | Single | 251 % | 286 % | 388 % | 377 % | 341 % |
| Medium dry c. / bulker, Alt. Bow | 14200 | IA | T | 400 | Single | 251 % | 286 % | 359 % | 403 % | 341 % |
| **Average** | | | | | | 273 % | 289 % | 415 % | 467 % | 442 % |
| **Average, without outliers** | | | | | | | **289 %** | **379 %** | **436 %** | **424 %** |

# 5 DISCUSSION

## 5.1 PERMANENT DEFORMATION ANALYSIS

Results of this study and the previous work reported in [2] are collected into Figure 16 to Figure 20.

It has been concluded together with Traficom that shell plate should always be designed using section 4.3 of the FSICR [3] and is not in scope of the new rules. This is because it is seen more beneficial to retain the simplicity of the current rules, and for shell plate, it is not seen that there would be significant benefit of doing analysis with alternative method.

Moreover, the shell plate is sensitive to load height and there might still be room for improvement regarding load height definition in the rules [13], which would then necessitate reconsideration of the criteria. Unlike shell plate, framing is relatively insensitive to load height and thus the current results are likely to be applicable even if the load height is changed in future rules.

Nevertheless, the capacity of the shell plating fulfilling requirements of the current rules, evaluated against the permanent deformation criteria defined in 3.2.3 are shown in Figure 16. As can be seen from Figure 16, some variation exist between the different example vessels, but as concluded in [2], generally the results of the new method align well with the current rule method.

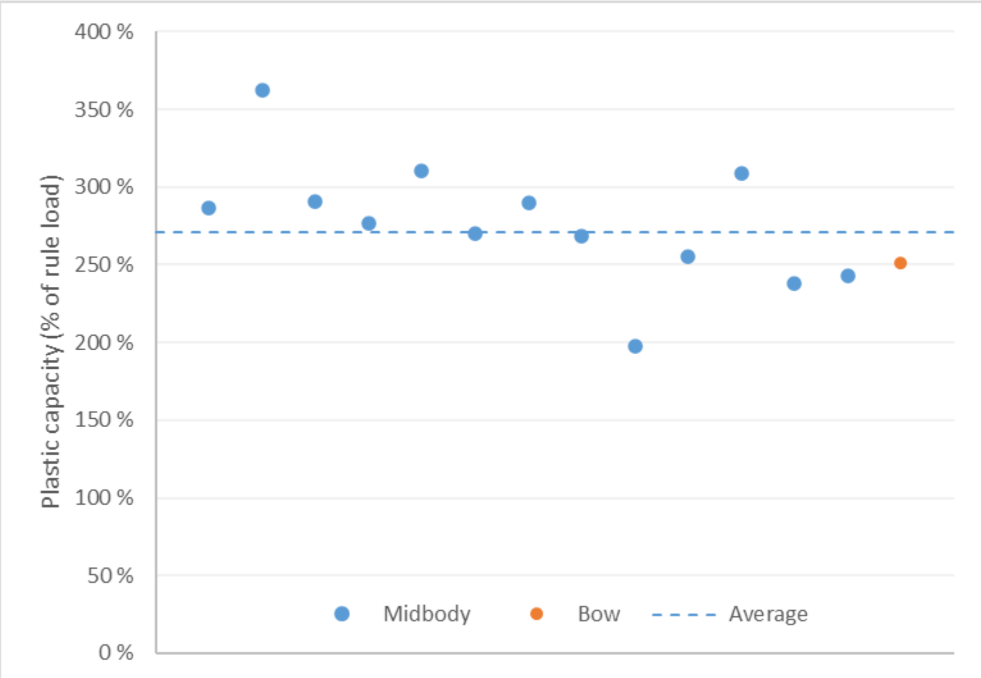


Figure 16 The load at which shell plate of each example vessel reached the permanent deformation limits defined in 3.2.3.

It was concluded together with Traficom that the aim of the new rules should be to retain equal level of strength to the current FSICR [3], as the current rules have long and favorable service experience. Thus, the required capacity for each structural element has been set to the average capacity of the example vessels studied in this study and HULLFEM II [2]. For the HULLFEM II vessels which have been reanalyzed in this study, the reanalyzed results have been used. The results for the bow have been weighted by factor of two when calculating the averages, as the same bow model would be applicable for both dry cargo vessel and bulk carrier, and as it is the only bow model.

The capacity of the frames fulfilling requirements of the current rules, evaluated against the permanent deformation criteria defined in 3.2.3 are shown in Figure 17. The average capacity of frames is 289 % of the current rule design load. This is rounded up to 2.90 as proposed requirement for frame capacity at permanent deformation limit defined in 3.2.3.

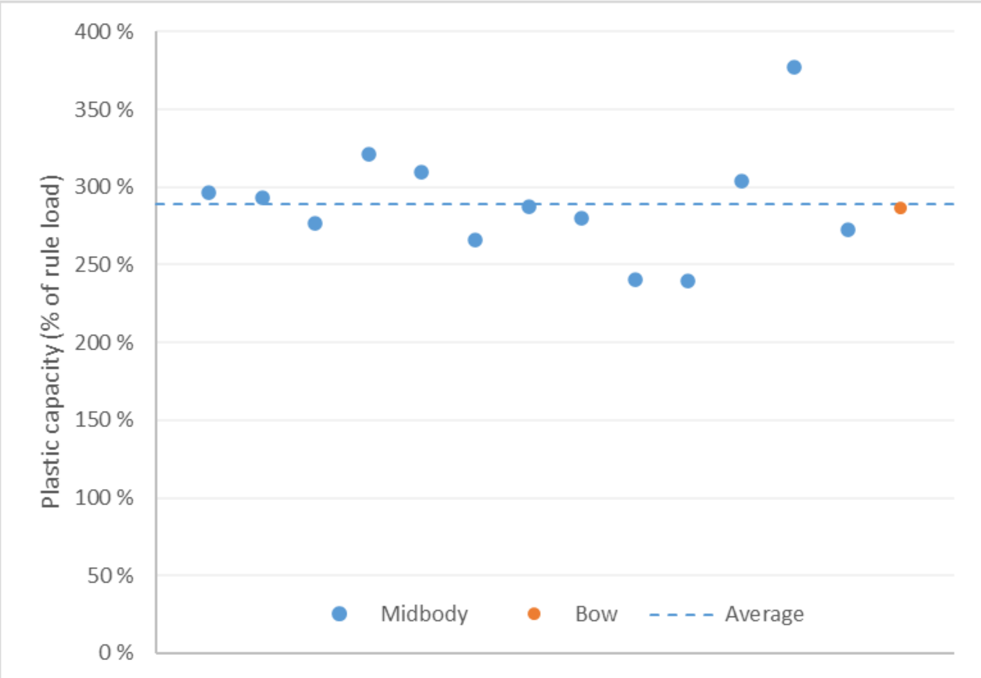


Figure 17 The load at which frames of each example vessel reached the permanent deformation limits defined in 3.2.3.

The capacity of the stringers fulfilling requirements of the current rules, evaluated against the permanent deformation criteria defined in 3.2.3 are shown in Figure 18. For some of the cases, namely the ones with double side construction where stringers are replaced by platforms, the open water rules and minimum thicknesses govern the design of the stringers, and the actual capacity exceeds the requirements of the ice class significantly. Thus, these are ignored in calculation of the average capacity and shown as outliers in Figure 18. The average capacity of stringers is 379 % of the current rule design load. This is rounded up to 3.80 as proposed requirement for stringer capacity at permanent deformation limit defined in 3.2.3.

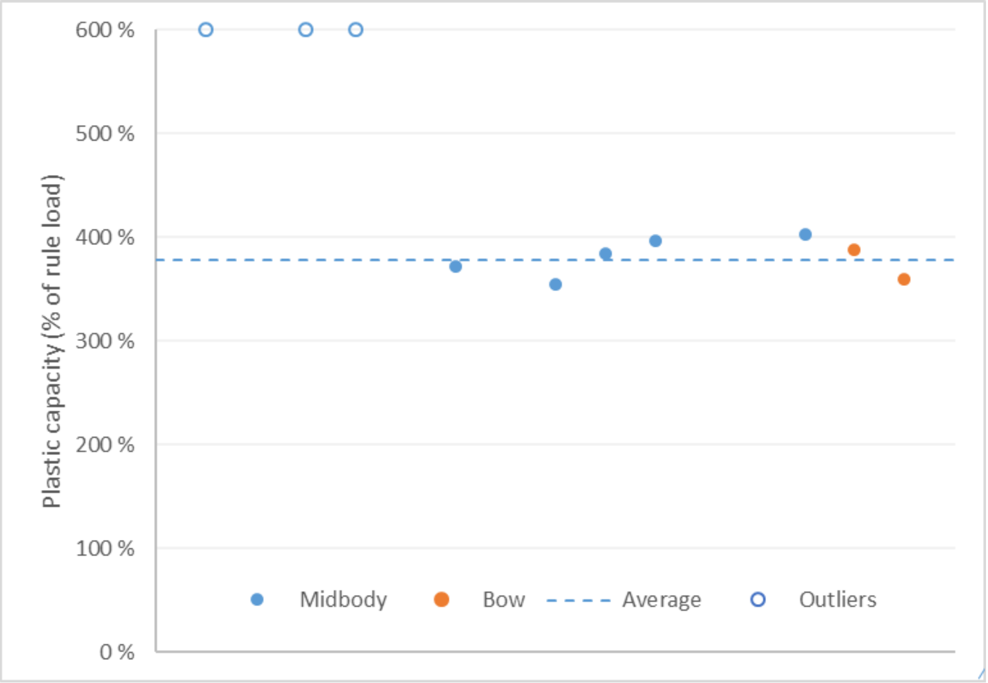


Figure 18 The load at which stringers of each example vessel reached the permanent deformation limits defined in 3.2.3.

The capacity of the web frames fulfilling the requirements of the current rules, evaluated against the permanent deformation criteria defined in 3.2.3 are shown in Figure 19. Similar to stringers, in some cases with double sided vessels, it was clear that the scantlings of the web frames were driven by the open water rules and minimum thicknesses rather than the requirements of ice class, and thus, these are ignored in calculation of the average capacity and similar to stringers, shown as outliers in Figure 19. The average capacity of the web frames is 436 % of the current rule design load.

However, this exceeds the upper limit of ice loads encountered on the Baltic Sea according to the damage statistics. This limit is discussed in more detail in 5.2. The average is 424 % of the current rule design load for the example vessels, which is rounded up to 4.25 for rule limit. Therefore, 4.25 times rule design load is the proposed requirement for web frame capacity at permanent deformation limit defined in 3.2.3.

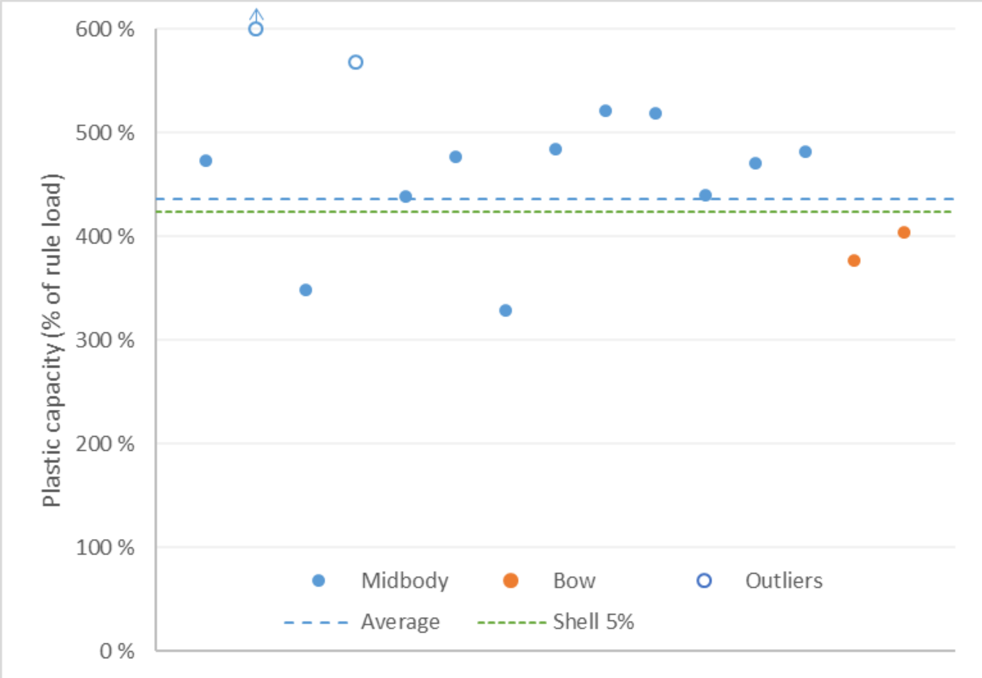


Figure 19 The load at which web frames of each example vessel reached the permanent deformation limits defined in 3.2.3.

## 5.2 ULTIMATE STRENGTH ANALYSIS

In 3.2.4 the ultimate ice load was defined as the load that causes 5 % of frame spacing permanent deformation on shell plate. This corresponds to the maximum measured ice damages [11], [12] on vessels designed to strength level equivalent to the current rules (i.e. according to FSICR 1985 or later).

The capacity of the shell plate fulfilling requirements of the current rules, evaluated against the ultimate deformation criteria defined in 3.2.4 are shown in Figure 20. One point is ignored as an outlier, as shown in Figure 20. On average, the load to cause 5 % of frame spacing permanent deformation on shell plating is 424 % of current rule design load. For rule proposal, this is rounded up to 4.25.

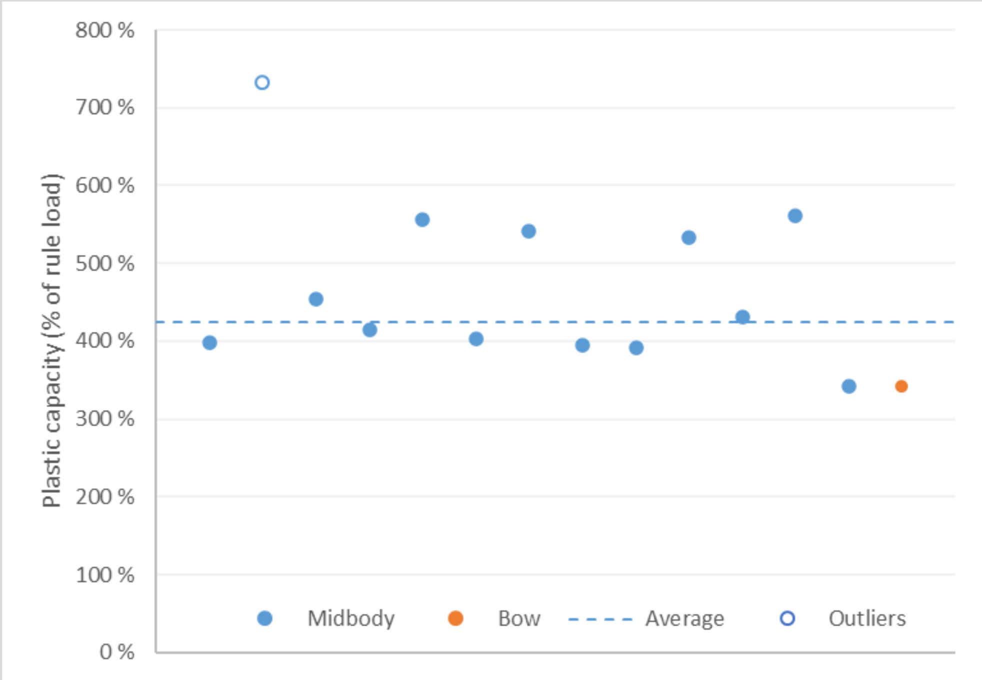


Figure 20 The load at which shell plating of each example vessel reached the ultimate deformation limit defined in 3.2.4.

## 5.3 TESTING OF PROPOSED CRITERIA

To assess how the example vessels would fare when evaluated against the criteria proposed in 5.1, calculated capacity of each was compared to the criteria. The results of this comparison are shown in Table 14. It should be noted that this comparison commits inverse crime, i.e. using the same analysis to both set and evaluate the criteria, and thus cannot be considered properly rigorous. However, given the effort required to model and analyze each vessel, having another fleet of example vessels just for this purpose would be not realistic. It was considered that even with its faults, this analysis is still useful way to visualize how the strength levels of the current and the proposed new rules compare, and how big changes would typically occur between the two.

As can be seen from Table 14, typically frames and stringers fall within ± 10 %, which can be considered well acceptable. There are few cases where frames have slightly larger differences. For stringers, most cases are remarkably close, and the ones with big differences are the cases where the scantlings are driven by other requirements than ice class, and therefore the design meets and exceeds requirements set by ice by a big margin.

For web frames, the variation is very much of same nature than for frames and stringers. Similar to stringers, there are two cases where the scantlings are driven by other considerations than ice class, and therefore the design meets and exceeds the requirements of ice class, leading to significant margin. The difference to stringers and frames is that in general, for most of the example vessels, the web frames have some capacity margin and could be made slightly lighter. This is due to the required strength level which is set at the maximum load calculated from the measured ice damages as calculated in 5.2, which slightly exceeds the average strength level required for web frames by the current rules as calculated in 5.1, and is therefore intentional.

In summary, it can be concluded that the variation between the current and the proposed alternative criteria is sufficiently small that it can be considered that both methods provide equivalent level of strength with acceptable accuracy.

Table 14 Capacity of each example ship compared to permanent deformation criteria set in 5.1.

| Frames | Stringers | Web frames |
|---|---|---|
| Pass 2 % | Pass 137 % | Pass 11 % |
| Pass 1 % | - | Pass 96 % |
| Fail -5% | Pass 163 % | Fail -18% |
| Pass 11 % | Pass 96 % | Pass 34 % |
| Pass 7 % | - | Pass 3 % |
| Fail -8% | Fail -2% | Pass 12 % |
| Fail -1% | - | Fail -23% |
| Fail -3% | Fail -7% | Pass 14 % |
| Fail -17% | Pass 1 % | Pass 23 % |
| Fail -17% | Pass 4 % | Pass 22 % |
| Pass 5 % | - | Pass 4 % |
| Pass 30 % | - | Pass 11 % |
| Fail -6% | Pass 6 % | Pass 13 % |
| Fail -1% | Pass 2 % | Fail -11% |
| Fail -1% | Fail -5% | Fail -5% |

# 6 CONCLUSIONS

In the first HULLFEM report [1], non-linear finite element method was chosen as the basis for developing direct calculation guidelines for the Finnish-Swedish Ice Class Rules. This was done to allow proper consideration of more varied structural configurations and to allow relaxation of the structural arrangement requirements, for example brackets. In the first report, the acceptance criteria were also outlined and tested on midships of three example vessels.

In the continuation project HULLFEM II [2], a wide array of typical Baltic Sea merchant vessel midships were analyzed, with the aim to cover all the typical ship types, sizes and structural configurations operating on the Baltic Sea.

In this final part of the project, HULLFEM III, a bow model was analyzed, acceptance criteria were refined, some of the earlier analysis was refined, and finally all results were collected together to form the basis for the rule proposal.

The bow analysis confirmed that the proposed acceptance criteria are applicable to both curved and prismatic hull regions, and the results obtained for the parallel midbody in HULLFEM II can be generalized for shaped regions (bow and stern).

Based on the research work done on these three projects, it is proposed that two criteria are sufficient to ensure equivalent level of strength and equivalent margin of safety against ice loads in both normal operation and during extreme ice loads encountered on the Baltic Sea, using non-linear finite element analysis as a tool. First criterion is that permanent deformation of the structure has to remain below 8 mm in any direction when the structure is subjected to plastic design ice load. Based on the results of the analyses made for the example vessels, this plastic design ice load should be set at 2.90 times the current rule design ice pressure for frames, 3.80 for stringers and 4.25 for web frames. The second criterion is that the load-deformation curve should have continuously positive slope up to ultimate ice load, which should be set at 4.25 times the current rule design ice pressure. It should be noted that these criteria are linked to the analysis method used and are recommended to be used only with similar type of analysis (i.e. finite element analysis with shell model, using plastic material and large displacement formulations).

Based on these studies, a rule draft shown in Appendix L has been written. The rule draft has been presented to Classification societies for commenting. The comments of the Classification societies have been used to refine the rules. As conclusion, the new rules are ready to be taken into use.

# 7 REFERENCES

[1] I. Perälä, K. Katajamäki and V. Valtonen, Direct calculation methods for ice strenghtened hulls in the Finnish-Swedish Ice Class Rules, VTT & Aker Arctic, 30.12.2022.

[2] V. Valtonen, "HULLFEM II - Direct calculation methods for ice strengthened hulls, part II," Aker Arctic, 2023.

[3] Traficom, Ice Class Regulations and the Application Thereof, Traficom, 2021.

[4] Dassault Systemes - SIMULIA, Abaqus user's manuals, elements, 2021.

[5] Lloyd's Register, Guidance Notes for Non-Linear Analysis for the Primary Support Structures for Polar Class Vessels, 2022.

[6] DNV, Class guideline CG-0127 Finite element analysis, August 2021.

[7] American Bureau of Shipping, Guidance note on nonlinear finite element analysis of marine and offshore structures, 2021.

[8] V. Valtonen, J. Bond and R. Hindley, "Improved method for non-linear FE analysis of Polar Class ship primary structures," *Marine Structures,* vol. 74, 2020.

[9] International Association of Classification Societies (IACS), Recommendation No.47 Shipbuilding and repair quality standard, IACS, rev. 8, 2017.

[10] Det Norske Veritas (DNV), Recommended practice C208 - Determination of structural capacity by non-linear finite element analysis method, DNV, October 2022.

[11] P. Kujala, Damage statistics of ice-strengthened ships in the Baltic Sea 1984-1987, Winter Navigation Research Board, Research report No.50.

[12] S. Hänninen, Incidents and accidents in winter navigation in the Baltic Sea, winter 2002-2003, Winter Navigation Research Board, Reserach report No. 54.

[13] K. Riska and J. Kämäräinen, "A review of ice loading and the evolution of the Finnish-Swedish ice class rules," *SNAME Transactions,* 2012.

| | |
|---|---|
| Design Phase | Copyright of Aker Arctic Technology Inc<br><br>All rights reserved. No part thereof may be disclosed, duplicated or in any other way made use of, except with prior approval of Aker Arctic Technology Inc<br><br>Aker Arctic |
| Confidentiality<br>Confidential | |
| Designer<br>Valtonen, V. | |
| Aker Arctic Design | Title<br>K560_A - Appendix L - Draft rules |
| Paper Size<br>A4 | |
| Document Date<br>2024-12-11 | |
| Pages<br>1 | Appendix to K560_A - HULLFEM III - Direct calculation methods for ice strengthened hulls, part III |

# PROPOSAL FOR DIRECT CALCULATION OF HULL STRUCTURES FOR THE FINNISH-SWEDISH ICE CLASS RULES

4rd draft, updated according to Traficom and Classification Society comments

## 4 HULL STRUCTURAL DESIGN

### 4.9 Non-linear finite element analysis

#### 4.9.1 General

This section describes an alternative method for determining the scantlings and construction of hull structures using non-linear finite element analysis. The analysis considers two sets of criteria. The permanent deformation analysis ensures that the permanent deformations in normal service do not exceed newbuilding tolerances. The ultimate strength analysis ensures that the structure has sufficient plastic reserve so that typical maximum ice loads encountered on the Baltic Sea do not lead to loss of load-carrying capacity resulting in major damage.

The method outlined in this section may be used for frames, ice stringers and web frames as an alternative to the methods outlined in sections 4.4, 4.5 and 4.6. Where there is deck, bulkhead or similar in lieu of a frame, stringer or web frame, the method outlined in this section may be applied for that member. The method outlined in this section shall not be used for calculating scantlings of shell plate or stem. Shell plate shall be designed according to section 4.3 and stem shall be designed according to section 4.7.

When frames are designed using the method outlined in this section, the requirements for brackets, end connections, tripping supports, and web thickness according to section 4.4.4 may be omitted when the acceptance criteria in section 4.9.3 are fulfilled. When there is a deck, bulkhead or similar in lieu of a frame, the requirements for plate thickness according to section 4.4.4 may be omitted when the acceptance criteria in section 4.9.3 are fulfilled. Welds and scallops shall be applied according to section 4.4.4.

When frames are designed using the method outlined in this section, stringers and web frames shall also be designed using the method outlined in this section.

When stringers are designed using the method outlined in this section, web frames shall also be designed using the method outlined in this section. Frames may be designed with the method outlined in this section or using section 4.4.

When web frames are designed using the method outlined in this section, frames and stringers may be designed with the method outlined in this section or by using sections 4.4. and 4.5.

For each hull region (bow, midbody, stern), the most onerous location(s) within the region shall be modelled and analysed. The analysis of the most onerous location(s) may be applied to all structures of the same hull region, providing that the structural arrangement and scantlings are similar.

### 4.9.2 Finite element model (FEM)

#### 4.9.2.1 Modelling and meshing

The analysis shall be done with a three-dimensional (3D) finite element model as described in section 4.9.2 of these rules.

The model shall be meshed with shell elements. In general, 4-node shell elements are recommended, but higher-order quadrilateral elements may be used. Triangular elements (3-node) may be used locally where necessary to achieve good quality mesh, but mesh should be quad-dominated. Beam elements shall not be used, except for pillars.

Model extents shall be sufficiently large to ensure that boundary conditions do not influence the deformation and stress distributions near the applied ice load patch. In general, at least two web frame spacings are recommended between the load patch edges and model boundaries. Plastic strain shall not be present at the model boundaries. In general, it is recommended that stresses at model boundaries are well below yield.

As far as practical, it is recommended that transverse bulkheads are used as model boundaries in the longitudinal direction.

In general, the model should extend vertically at least from the main deck to the tank top, or if there is no tank top, to the bottom. In case either of these is close to the ice belt, the model should be extended to include the bottom and/or the next deck above main deck (if any). In all cases, the model extent should exceed the vertical extent of ice frames as given in section 4.4.1 at least by one stringer spacing for transversally framed ships and one web frame spacing for longitudinally framed ships. Two spacings are generally recommended.

In general, the model should extend from the ship side to centreline in the athwartships direction. For symmetric ships, it is sufficient to model only one side of the ship. Appropriate boundary conditions should be applied at the centreline.

Mesh dimensions shall be chosen to fulfil following criteria:

- On stiffened plate panels, there should be at least 8 elements between stiffeners.
- On webs of frames, there should be at least 3, preferably 4, elements along the web height.
- In general, mesh size on frames, stringers and web frames should be similar to shell plate. Smaller elements may be used where advantageous.
- In ice strengthened structure (structure covered by section 4), mesh size should be between *t* and 10 *t*, where *t* is the plate thickness.

Gross thicknesses shall be used in general. Shell plate thickness within the ice belt shall be reduced by the corrosion and abrasion margin $t_c$ given in section 4.3.2.

The model should include sufficient level of detail to represent the behaviour of the structure accurately. Stiffener flanges should be modelled with shell elements. Brackets, including flanges, should be modelled with shell elements. Manholes and other large cutouts should be modelled with actual geometry. Web stiffeners for large members and tripping brackets should be modelled with shell elements. Bulb profiles may be modelled as equivalent L-profiles.

Drain holes, scallop holes, welds and similar small details may be omitted.

When a frame is running through the supporting structure and has both sides of web effectively connected to the supporting structure (by lug, collar plate or direct welding, as shown in Figure 4-5 a, b and c) as described in 4.4.4.1, the frame cutout need not be modelled. If lugs are omitted for the ice frames, as shown in Figure 4-5 d, the frame cutout shall be modelled.

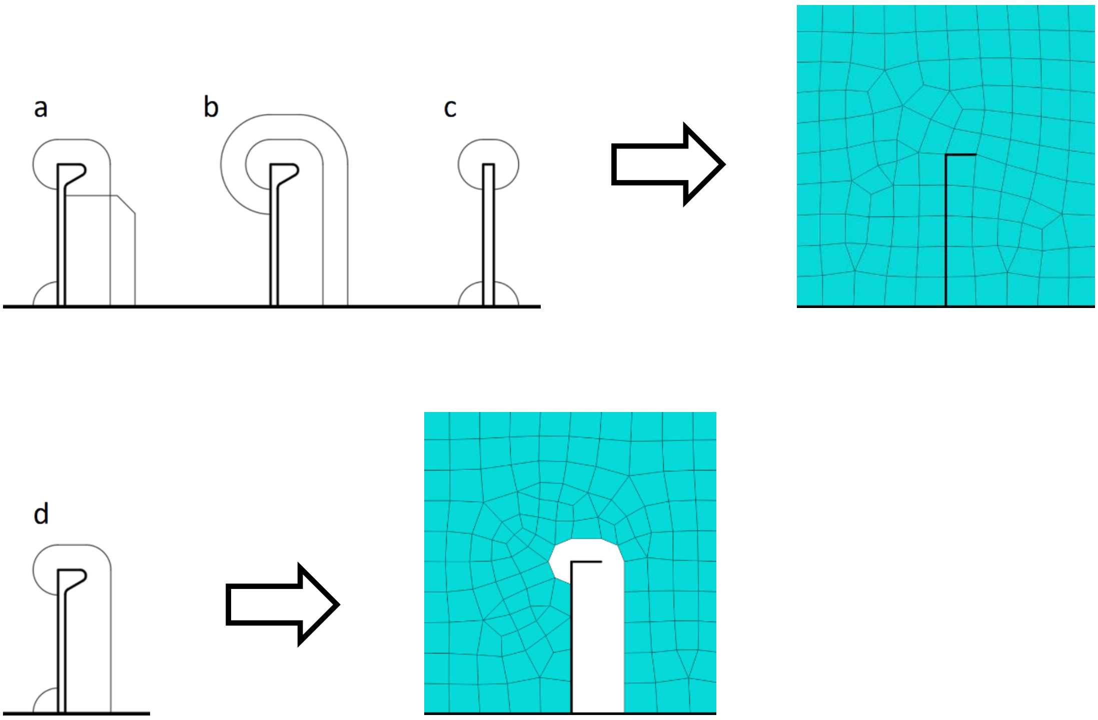


*Figure 4-5 Modelling of cutouts for ice frames with cutout and lug (a), watertight collar (b), web directly welded to crossing member on both sides (c) and cutout connected to crossing member only on one side (d).*

#### 4.9.2.2 Material model

The material model shall consider plasticity and be able to represent the non-linear behaviour of the material.

The material model may be either bilinear or a more accurate plastic material model approved by the Classification Society. For a bilinear material model, a tangent modulus $E_T$ of 1000 MPa should be used in general. Where a higher value is used for the tangent modulus for a bilinear model, it shall be justified. Unloading shall be done along the elastic curve. A bilinear material model is illustrated in Figure 4-6.

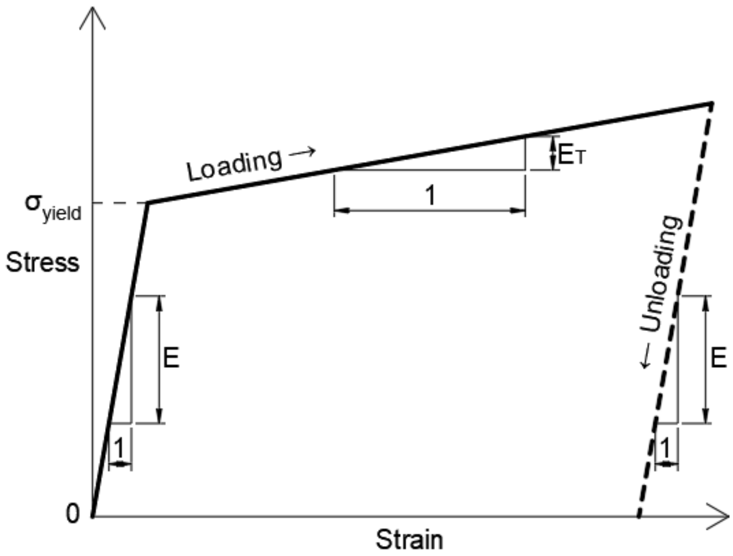


*Figure 4-6 Bilinear material model and tangent modulus $E_T$.*

#### 4.9.2.3 Boundary conditions

Boundary conditions representing the support provided by the structure at the boundary shall be applied on all model edges. The boundary conditions (fixed, pinned, symmetry, free, other) shall be chosen to represent the support provided by the actual structure at the boundary as relevant.

In general, bulkheads and similar plate structures can be considered to provide translational restraint in the respective plane. Fixed boundary conditions (both translational and rotational restraint) may only be used when the structure at the boundary provides sufficient rotational restraint and rigidity.

#### 4.9.2.4 Design loads

The ice load shall be applied as a pressure load. The shape of the pressure load shall be a rectangular patch. The load patch height is the design ice load height $h$ according to Table 4-1. The load patch width is the design ice load length $l_a$ according to Table 4-4. The load patch shall be oriented parallel to the waterline.

No other loads (static pressure, wave, gravity, etc.) are to be applied to the model.

The load patch may be aligned with the mesh. Dimensions $h$ and $l_a$ may be rounded to align with the closest nodes. If the patch size is adjusted to align with the mesh, the design ice pressure shall be adjusted so that the total force on the load patch remains constant.

The load shall be applied to the model in two separate analyses. For permanent deformation analysis, the design ice load is to be applied and removed, after which the model is assessed with the acceptance criteria given in 4.9.3.1. For ultimate strength analysis, the ultimate load is applied, after which the model is assessed with the acceptance criteria given in 4.9.3.2. The load application is illustrated in Figure 4-7.

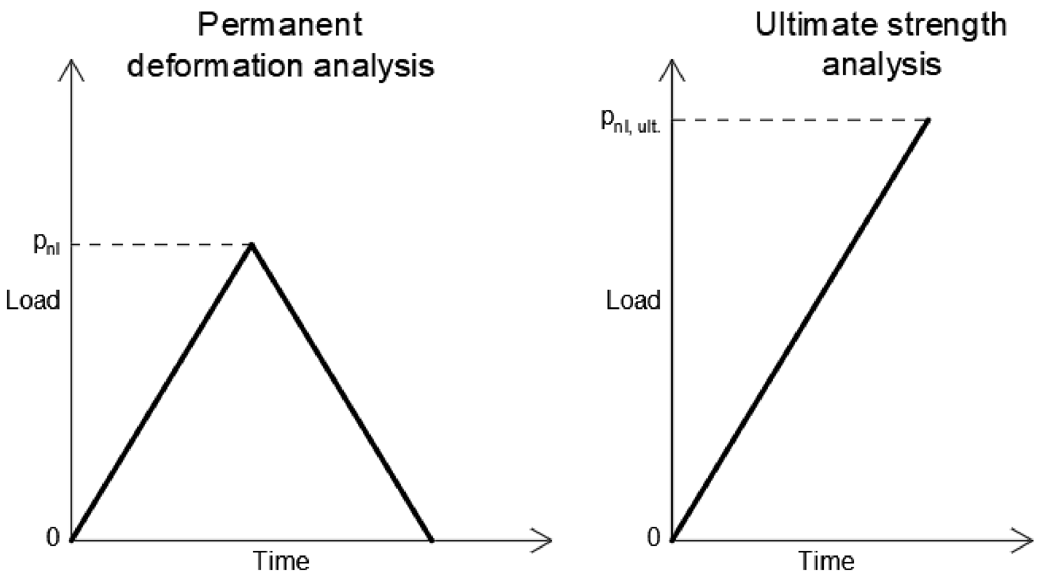


*Figure 4-7 Load history for permanent deformation analysis and ultimate strength analysis.*

The design ice pressure to be applied to the model for determining permanent deformation shall be

$$p_{nl} = f_{13} \frac{h\, l_a}{h_m\, l_m} p, \tag{4.18}$$

where

| | |
|---|---|
| $f_{13}$ | is a factor for non-linear capacity as given in Table 4-9 |
| $h$ | is the design ice load height as given in Table 4-1 |
| $h_m$ | is the load patch height in the model |
| $l_a$ | is the design ice load width as given in Table 4-4 |
| $l_m$ | is the load patch width in the model |
| $p$ | is the design ice pressure as given in section 4.2.2 |

The ultimate ice pressure to be applied to the model for determining ultimate strength shall be

$$p_{nl,ult.} = f_{14} \frac{h\, l_a}{h_m\, l_{a,m}} p,$$

where

| | |
|---|---|
| $f_{14}$ | is the factor for ultimate strength as given in Table 4-9. |

*Table 4-9 Values for non-linear capacity factors $f_{13}$ and $f_{14}$ for different structural elements.*

| Structural member | $f_{13}$ | $f_{14}$ |
|---|---|---|
| Frames (section 4.4) | 2.90 | 4.25 |
| Ice stringers (section 4.5) | 3.80 | 4.25 |
| Web frames (section 4.6) | 4.25 | 4.25 |

#### 4.9.2.5 Load cases

The ice load shall be applied at locations where capacity of the structure is minimal. For all members, the load patch shall be applied at the centre of effective span. Additionally, the load patch shall be applied in way of any manholes or other large cutouts in member web. The ice load need not to be applied outside vertical extension defined for plating in Table 4-5.

In the vertical direction, the load patch shall be applied centred at UIWL, at 0.5 $h_i$ below LIWL, and at any location which may be considered more onerous. In particular, the load patch shall be applied at the centre of the effective span of transverse frames and web frames. For web frames supporting stringers, the load patch shall be applied at each stringer within the ice belt. For stringers and longitudinal frames, the load patch shall be centred on the member under consideration.

Horizontally, the load patch shall be applied centred on the member under consideration, and at any location which may be considered more onerous. In particular, the load patch shall be applied at the centre of the effective span of longitudinal frames and stringers. For transverse frames and web frames, the load patch shall be centred on the member under consideration.

Where there is a deck in lieu of a stringer or a longitudinal frame, similar load cases should be applied as for a stringer. Where there is a bulkhead in lieu of a frame or a web frame, similar load cases should be applied as for a web frame.

Load patch locations for typical transverse framing system are given in Table 4-10 and for typical longitudinal framing system in Table 4-11. For non-typical framing systems, load patch locations are to be developed on a case-by-case basis using Table 4-10 and Table 4-11 as a basis. Where any other location is considered more onerous than those given in these tables, it shall be analysed in addition.

*Table 4-10 Load patch locations for typical transversal framing system.*

| | Vertical | Horizontal |
|---|---|---|
| Transverse frame | - at UIWL<br>- at 0.5 $h_i$ below LIWL<br>- at centre of effective span<br>- at ends of effective span, when end connection not according to 4.4.4 | - centred on frame |
| Stringer | - centred on stringer | - at centre of effective span<br>- in way of manholes or large cutouts |
| Web frame supporting stringers | - at UIWL<br>- at 0.5 $h_i$ below LIWL<br>- at centre of effective span<br>- at each stringer within ice belt<br>- in way of manholes or large cutouts | - centred on web frame |

*Table 4-11 Load patch locations for typical longitudinal framing system.*

| | Vertical | Horizontal |
|---|---|---|
| Longitudinal frame | - centred on frame | - at centre of effective span<br>- at ends of effective span, when end connection not according to 4.4.4 |
| Web frame | - at UIWL<br>- at 0.5 $h_i$ below LIWL<br>- at centre of effective span<br>- at each end of effective span<br>- in way of manholes or large cutouts | - centred on web frame |

#### 4.9.2.6 Solution

The analysis may be undertaken with an implicit or explicit solver.

The analysis shall consider geometric non-linearities, including buckling and tripping. In practice, this means that large-displacement formulations shall be used.

Load shall be applied incrementally. The increments shall be sufficiently small to guarantee sufficient accuracy. In particular, when buckling is relevant for the structural members under consideration, sufficiently small load increments should be used.

In general, stabilization / dampening should not be applied. In case stabilization / dampening is applied, it shall be demonstrated that it does not have an appreciable effect on the calculated capacity.

#### 4.9.3 Acceptance criteria

The acceptance criteria shall be applied to all structural members where this analysis is used in lieu of the requirements of sections 4.3 to 4.7 and to any structure supporting those structural members. For shell plating and any other structural members which are designed according to sections 4.3 to 4.7, the acceptance criteria defined in this section need not to be fulfilled.

##### 4.9.3.1 Permanent deformation analysis

After the design ice pressure $p_{nl}$ defined in section 4.9.2.4 has been applied and removed, the permanent deformation of any part of any member shall not exceed 8 mm in any direction. The deformation shall be measured as total deformation, i.e. relative to original position, not deformation relative to supporting member.

Alternatively, the 8 mm limit value may be replaced by the approved newbuilding tolerances of the Classification Society.

##### 4.9.3.2 Ultimate strength analysis

The load-deformation curve shall have a positive slope at all points from zero up to the ultimate ice pressure $p_{nl,ult.}$ defined in section 4.9.2.4.

It is to be noted that at the ultimate ice pressure $p_{nl,ult.}$, local buckling, tripping and large deformations are permitted, provided that the abovementioned criteria are met.